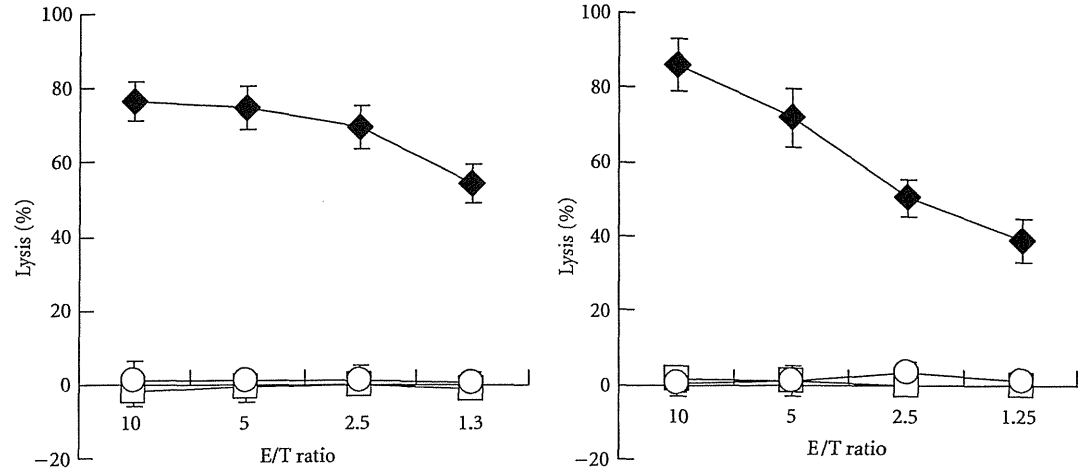

FIGURE 5: Cytotoxic activity of CTL clones against peptide-pulsed TISI cells. Cytotoxic activity of CDH3-10-807 peptide-specific CTL clone (a) and KIF20A-10-66 peptide-specific CTL clone (b) against HLA-A*2402-positive TISI cells pulsed with respective peptide (close diamond), HIV-A24 peptide (open square), or TISI cells without peptide pulse (open circle). E/T ratio, effector cell (CTL clone)/target cell (TISI cell) ratio. Similar results were obtained in three independent experiments using same CTL clone and in independent experiments using other CTL clones.

IFN-γ specifically responding to the stimulator cells pulsed with the respective peptide, but not HIV-A24 peptide (Figures 2(a)–2(d)).

*3.3. Recognition of Cells Endogenously Expressing Both HLA-A*2402 and Respective Protein by Peptide-Specific CTL Clones.* We then examined that the established peptide-specific CTL clones can recognize cells that express HLA-A*2402 and the target proteins. COS7 cells were transfected with plasmid designed to express HLA-A*2402 molecule and/or that to express the full length protein of CDH3 or KIF20A. We confirmed expression of these proteins by western blotting (data not shown). CDH3-10-807 peptide responding CTL clone substantially produced IFN-γ when exposed to COS7 cells that expressing both HLA-A*2402 and CDH3, but not COS7 cells that expressing either HLA-A*2402 or CDH3 (Figure 3(a)). Similarly, KIF20A-10-66 peptide responding CTL clone produced significant amount of IFN-γ when exposed to COS7 cells that expressing both HLA-A*2402 and KIF20A, but not COS7 cells that expressing either HLA-A*2402 or KIF20A (Figure 3(b)). Both CTL clones also produced IFN-γ responding to COS7 cells, which transfected with pIRES-vector containing both HLA-A*2402 and respective oncogene (data not shown). On the other hand, CTL clones responding to KIF20A-9-305 peptide or KIF20A-10-304 peptide did not produce IFN-γ when exposed to COS7 cells expressing both HLA-A*2402 and KIF20A (data not shown). Only CDH3-10-807 peptide and KIF20A-10-66 peptide, but not other candidate peptides, were able to induce CTL responding to COS7 cells expressing HLA-A*2402 and CDH3 or KIF20A, albeit we have tried several times using PBMC derived from different healthy donors (data not shown).

3.4. Peptide-Specific T Cell Receptor Expression. Expression of CDH3-10-807/HLA-A*2402- or KIF20A-10-66/HLA-A*2402-specific T cell receptor (TCR) was examined using CDH3-10-807/MHC-dextramer-PE or KIF20A-10-66/MHC-dextramer-PE. Significant population of $CD3^+$ $CD8^+$ cells, but not $CD3^+$ $CD8^-$ cells, expressed CDH3-10-807/HLA-A*2402- or KIF20A-10-66/HLA-A*2402- specific TCR after expansion of cells obtained by "*in vitro* induction of peptide-specific CTL" (Figures 4(a) and 4(b)). As expected, CTL clones established by CDH3-10-807 peptide- or KIF20A-10-66 peptide-pulsed cells were CD8 positive and expressed respective peptide/HLA-A*2402-specific TCR (Figures 4(c) and 4(d)).

3.5. Cytotoxic Activity of CTLs. We also examined cytotoxic activity of CTL clones. CDH3-10-807 or KIF20A-10-66 peptide-specific CTL clone demonstrated cytotoxic activity against HLA-A*2402-positive TISI cells when respective peptide was pulsed, but not when HIV-A24 peptide was pulsed or peptide was not pulsed (Figures 5(a) and 5(b)). These results suggested that CDH3-10-807 or KIF20A-10-66 peptide-specific CTL clone specifically exerted cytotoxic activity responding to respective epitope peptide binding to HLA-A*2402 on cells.

We, then, finally examined the cytotoxic activity against cancer cells, which endogenously expressed CDH3 or KIF20A gene. Expression of CDH3 protein was confirmed in HLA-A*2402-positive PK-45P cells and HLA-A*2402-negative H358 cells, but HLA-A*2402-positive MiaPaca-2 cells did not express CDH3 (Figure 6(a)). CDH3-10-807 peptide-specific CTL clone exerted significant cytotoxic activity against CDH3-expressing HLA-A*2402-positive PK-45P cells, but not H358 or MiaPaca-2 cells (Figure 6(b)).

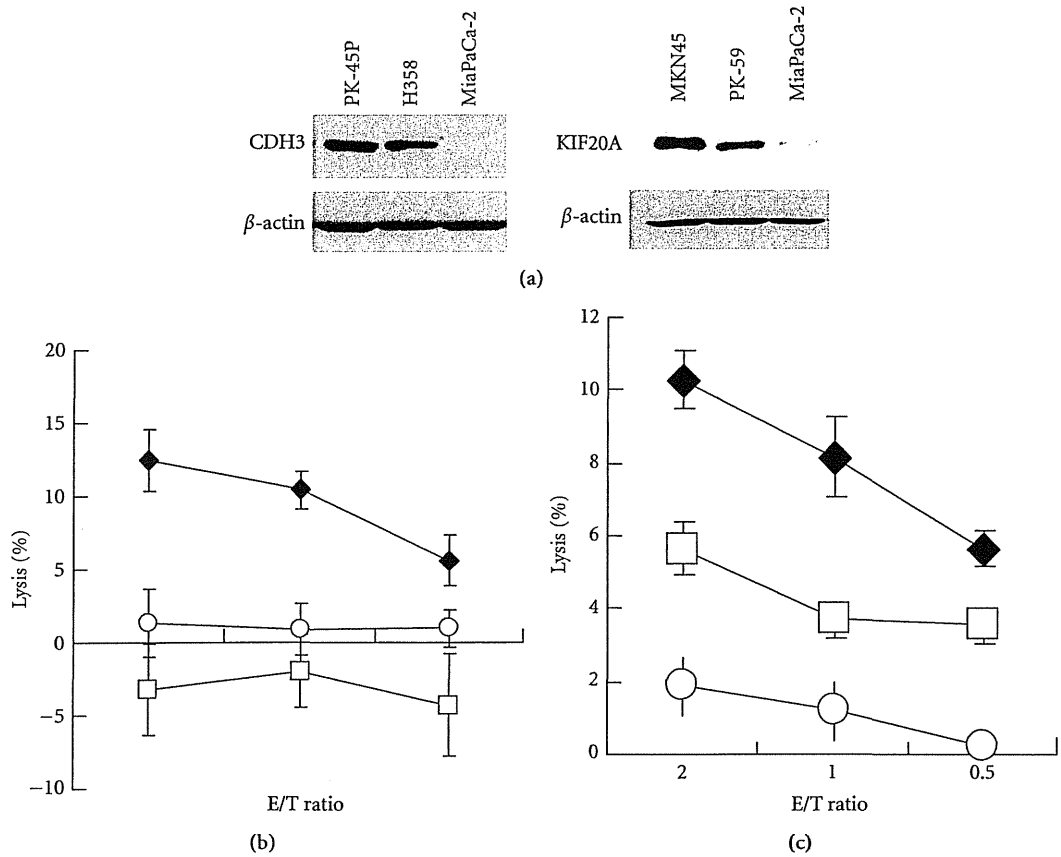

FIGURE 6: Cytotoxic activity against tumor cells expressing respective gene. (a) The expression of CDH3 and KIF20A protein in tumor cells used in cytotoxic assay. (b) Cytotoxic activity of CDH3-10-807 peptide-specific CTL clone against CDH3-expressing HLA-A*2402-positive PK-45P cells (closed diamond), CDH3-expressing HLA-A*2402-negative H358 cells (open square), or MiaPaCa-2 cells (open circle). Cytotoxicity against PK-45P cells was significantly higher than those against other cells. (c) Cytotoxic activity of KIF20A-10-66 peptide-specific CTL clone against KIF20A-expressing HLA-A*2402-positive MKN-45 cells (closed diamond), KIF20A-expressing HLA-A*2402-negative PK-59 cells (open square), or MiaPaCa-2 cells (open circle). Cytotoxicity against MKN-45 cells or PK-59 cells are significantly higher than that against MiaPaCa-2 cells, although cytotoxic activity against PK-59 cells was significantly lower compared with that against MKN-45 cells. E/T ratio, effector cell (CTL clone)/target cell (tumor cell) ratio. Similar results were obtained in three independent experiments using same CTL clone and in independent experiments using other CTL clones.

Expression of KIF20A protein was confirmed in HLA-A*2402-positive MKN-45 cells and HLA-A*2402-negative PK-59 cells, but HLA-A*2402-positive MiaPaca-2 cells did not express KIF20A (Figure 6(a)). KIF20A-10-66 peptide-specific CTL clone exerted significant cytotoxic activity against KIF20A-expressing HLA-A*2402-positive MKN-45 cells, but not MiaPaca-2 cells (Figure 6(c)). KIF20A-10-66 peptide-specific CTL clone demonstrated cytotoxic activity against KIF20A-expressing HLA-A*2402-negative PK-59 cells; however, this cytotoxicity was always less when compared with that against KIF20A-expressing HLA-A*2402-positive MKN-45 cells (Figure 6(c) and data not shown).

No homologous sequence to CDH3-10-807 peptide or KIF20A-10-66 peptide was demonstrated by the homology research using the BLAST algorithm http://blast.ncbi.nlm.nih.gov/Blast.cgi (data not shown), suggesting that these peptide would be the unique epitope peptide presented on HLA-A*2402 of CDH3 or KIF20A-expressing cells.

Taken together, presented results suggested that CDH3-10-807 peptide-specific or KIF20A-10-66 peptide-specific CTLs exert potent IFN-γ production and cytotoxic activity specifically responding to HLA-A*2402-positive cancer cells expressing CDH3 or KIF20A, respectively.

4. Discussion

Pancreatic cancer is one of the most malignant cancers, since 5-year survival rate is only 5% and the therapeutic modalities are very limited [26, 27]. Both CDH3 and KIF20A were upregulated in the majority of pancreatic cancers and have oncogenic functions [15, 16]. Thus, CDH3 and KIF20A would be promising target molecules to develop novel therapeutic strategies for pancreatic cancer. Hence, we identified HLA-A*0201-restricted peptides derived from CDH3 and KIF20A [28, 29].

In present study, we successfully identified HLA-A*2402-restricted novel epitope peptides derived from both CDH3 and KIF20A and demonstrated that these peptides could induce specific CTLs producing potent amount of IFN-γ and

exert cytotoxic activity. Established CDH3-10-807-specific CTL clones or KIF20A-10-66-specific CTL clones responded to CDH3- or KIF20A-introduced COS7 cells as well as CDH3 or KIF20A endogenously expressing cancer cells (PK-45P or MKN-45) in HLA-A24-restricted manner. These results indicated that induction of CDH3-10-807-specific CTLs or KIF20A-10-66-specific CTLs would exert antitumor effect against pancreatic cancers in HLA-A24-positive patients.

Predicted binding score of KIF20A-10-66 peptide to HLA-A*2402 was relatively low when compared with that of CDH3-10-807 peptide. We previously reported epitope peptides derived from RNF43 and IMP-3, and those peptides also have low affinity to HLA molecule [22, 24]. Interestingly, both peptides have been already applied for clinical trials as peptide-based immunotherapy and CTL were obtained in many cancer patients [11, 12]. These results suggested that some peptides possibly induce CTLs albeit binding score was low by BIMAS prediction and KIF20A-10-66 peptide, as well as CDH3-10-807 peptide, possibly induces CTL in cancer patients.

Recent improvement and development of cancer therapies, including combined treatments of standard therapies (chemotherapy, radiotherapy, and surgical resection), substantially improved the survival of advanced cancer patients [27]. However, unfavorable adverse events are still often observed. On the other hand, immune therapies inducing cancer-cell-specific CTLs are now developed to improve the efficacy against cancers and the quality of life of patients. Ongoing several clinical trials using epitope peptides derived from TAA have been proving the evidence that CTL-inducing therapies are much less harmful to the patients [10–12]. However, efficacy of some vaccine therapy trials is still limited mainly due to the development of escaping variant cancer cells that lost targeted TAA expression during the treatment [30]. Therefore, it is generally thought that the therapeutic efficacy would be improved when the origin of vaccinated peptide is functionary essential molecule for cancer cell survival, proliferation, and/or motility. We have been screening epitope peptides derived from cancer-specific genes and reported several epitope peptides, which can elicit specific CTL responses [21–24]. Some of these peptides have been already applied for translational researches of multipeptide vaccine to treat esophageal cancer and colorectal cancer [11, 12]. Moreover, multiple-antigen vaccine therapy was suggested to more effectively hinder escape mechanisms in the guidance from Food and Drug Administration (Guidance for Industry: Clinical Considerations for Therapeutic Cancer Vaccines). Thus, we believe that identification of CTL-inducible epitope peptides derived from several molecules that play critical roles in various types of cancer is important to develop multipeptide cocktail, and that resulted in the improvement of efficacy of CTL-inducing cancer therapies.

Presented results demonstrated that CDH3-10-807 peptide and KIF20A-10-66 peptide pulsed DCs induced specific CTL to possibly exert antitumor effect. The immunogenicity of CDH3-10-807 peptide and KIF20A-10-66 peptide should be examined in patients bearing these genes-expressing cancers, and we are now going to conduct clinical trials.

References

[1] T. Boon, "Tumor antigens recognized by cytolytic T lymphocytes: present perspectives for specific immunotherapy," *International Journal of Cancer*, vol. 54, no. 2, pp. 177–180, 1993.

[2] T. Boon and P. Van der Bruggen, "Human tumor antigens recognized by T lymphocytes," *Journal of Experimental Medicine*, vol. 183, no. 3, pp. 725–729, 1996.

[3] P. van der Bruggen, C. Traversari, P. Chomez et al., "A gene encoding an antigen recognized by cytolytic T lymphocytes on a human melanoma," *Science*, vol. 254, no. 5038, pp. 1643–1647, 1991.

[4] V. Brichard, A. Van Pel, T. Wolfel et al., "The tyrosinase gene codes for an antigen recognized by autologous cytolytic T lymphocytes on HLA-A2 melanomas," *Journal of Experimental Medicine*, vol. 178, no. 2, pp. 489–495, 1993.

[5] Y. Kawakami, S. Eliyahu, K. Sakaguchi et al., "Identification of the immunodominant peptides of the MART-1 human melanoma antigen recognized by the majority of HLA-A2-restricted tumor infiltrating lymphocytes," *Journal of Experimental Medicine*, vol. 180, no. 1, pp. 347–352, 1994.

[6] Y. T. Chen, M. J. Scanlan, U. Sahin et al., "A testicular antigen aberrantly expressed in human cancers detected by autologous antibody screening," *Proceedings of the National Academy of Sciences of the United States of America*, vol. 94, no. 5, pp. 1914–1918, 1997.

[7] S. R. Reynolds, A. Zeleniuch-Jacquotte, R. L. Shapiro et al., "Vaccine-induced $CD8^+$ T-cell responses to MAGE-3 correlate with clinical outcome in patients with melanoma," *Clinical Cancer Research*, vol. 9, no. 2, pp. 657–662, 2003.

[8] S. A. Rosenberg, J. C. Yang, D. J. Schwartzentruber et al., "Recombinant fowlpox viruses encoding the anchor-modified gp100 melanoma antigen can generate antitumor immune responses in patients with metastatic melanoma," *Clinical Cancer Research*, vol. 9, no. 8, pp. 2973–2980, 2003.

[9] G. Pecher, A. Häring, L. Kaiser, and E. Thiel, "Mucin gene (MUC1) transfected dendritic cells as vaccine: results of a phase I/II clinical trial," *Cancer Immunology, Immunotherapy*, vol. 51, no. 11-12, pp. 669–673, 2002.

[10] M. Miyazawa, R. Ohsawa, T. Tsunoda et al., "Phase I clinical trial using peptide vaccine for human vascular endothelial growth factor receptor 2 in combination with gemcitabine for patients with advanced pancreatic cancer," *Cancer Science*, vol. 101, no. 2, pp. 433–439, 2010.

[11] K. Kono, Y. Mizukami, Y. Daigo et al., "Vaccination with multiple peptides derived from novel cancer-testis antigens can induce specific T-cell responses and clinical responses in advanced esophageal cancer," *Cancer Science*, vol. 100, no. 8, pp. 1502–1509, 2009.

[12] K. Okuno, F. Sugiura, J. I. Hida et al., "Phase I clinical trial of a novel peptide vaccine in combination with UFT/LV for metastatic colorectal cancer," *Experimental and Therapeutic Medicine*, vol. 2, no. 1, pp. 73–79, 2011.

[13] M. Palmer, J. Parker, S. Modi et al., "Phase I study of the BLP25 (MUC1 peptide) liposomal vaccine for active specific immunotherapy in stage IIIB/IV non-small-cell lung cancer," *Clinical Lung Cancer*, vol. 3, no. 1, pp. 49–57, 2001.

[14] T. Nakamura, Y. Furukawa, H. Nakagawa et al., "Genome-wide cDNA microarray analysis of gene expression profiles in pancreatic cancers using populations of tumor cells and normal ductal epithelial cells selected for purity by laser microdissection," *Oncogene*, vol. 23, no. 13, pp. 2385–2400, 2004.

[15] K. Taniuchi, H. Nakagawa, M. Hosokawa et al., "Overexpressed P-cadherin/CDH3 promotes motility of pancreatic cancer cells by interacting with p120ctn and activating Rho-family GTPases," *Cancer Research*, vol. 65, no. 8, pp. 3092–3099, 2005.

[16] K. Taniuchi, H. Nakagawa, T. Nakamura et al., "Down-regulation of RAB6KIFL/KIF20A, a kinesin involved with membrane trafficking of discs large homologue 5, can attenuate growth of pancreatic cancer cell," *Cancer Research*, vol. 65, no. 1, pp. 105–112, 2005.

[17] M. Takeichi, "The cadherins: cell-cell adhesion molecules controlling animal morphogenesis," *Development*, vol. 102, no. 4, pp. 639–655, 1988.

[18] F. Lai, A. A. Fernald, N. Zhao, and M. M. Le Beau, "cDNA cloning, expression pattern, genomic structure and chromosomal location of RAB6KIFL, a human kinesin-like gene," *Gene*, vol. 248, no. 1-2, pp. 117–125, 2000.

[19] Y. Ikeda-Moore, H. Tomiyama, K. Miwa et al., "Identification and characterization of multiple HLA-A24-restricted HIV-1 CTL epitopes: strong epitopes are derived from V regions of HIV-1," *Journal of Immunology*, vol. 159, no. 12, pp. 6242–6252, 1997.

[20] E. Celis, V. Tsai, C. Crimi et al., "Induction of anti-tumor cytotoxic T lymphocytes in normal humans using primary cultures and synthetic peptide epitopes," *Proceedings of the National Academy of Sciences of the United States of America*, vol. 91, no. 6, pp. 2105–2109, 1994.

[21] H. Ishizaki, T. Tsunoda, S. Wada, M. Yamauchi, M. Shibuya, and H. Tahara, "Inhibition of tumor growth with antiangiogenic cancer vaccine using epitope peptides derived from human vascular endothelial growth factor receptor 1," *Clinical Cancer Research*, vol. 12, no. 19, pp. 5841–5849, 2006.

[22] N. Uchida, T. Tsunoda, S. Wada, Y. Furukawa, Y. Nakamura, and H. Tahara, "Ring finger protein 43 as a new target for cancer immunotherapy," *Clinical Cancer Research*, vol. 10, no. 24, pp. 8577–8586, 2004.

[23] S. Wada, T. Tsunoda, T. Baba et al., "Rationale for antiangiogenic cancer therapy with vaccination using epitope peptides derived from human vascular endothelial growth factor receptor 2," *Cancer Research*, vol. 65, no. 11, pp. 4939–4946, 2005.

[24] T. Suda, T. Tsunoda, Y. Daigo, Y. Nakamura, and H. Tahara, "Identification of human leukocyte antigen-A24-restricted epitope peptides derived from gene products upregulated in lung and esophageal cancers as novel targets for immunotherapy," *Cancer Science*, vol. 98, no. 11, pp. 1803–1808, 2007.

[25] K. Takeda, N. Yamaguchi, H. Akiba et al., "Induction of tumor-specific T cell immunity by anti-DR5 antibody therapy," *Journal of Experimental Medicine*, vol. 199, no. 4, pp. 437–448, 2004.

[26] A. Sultana, C. Tudur Smith, D. Cunningham et al., "Systematic review, including meta-analyses, on the management of locally advanced pancreatic cancer using radiation/combined modality therapy," *British Journal of Cancer*, vol. 96, no. 8, pp. 1183–1190, 2007.

[27] A. Jemal, R. Siegel, E. Ward, Y. Hao, J. Xu, and M. J. Thun, "Cancer statistics, 2009," *CA Cancer Journal for Clinicians*, vol. 59, no. 4, pp. 225–249, 2009.

[28] K. Imai, S. Hirata, A. Irie et al., "Identification of a novel tumor-associated antigen, cadherin 3/P-cadherin, as a possible target for immunotherapy of pancreatic, gastric, and colorectal cancers," *Clinical Cancer Research*, vol. 14, no. 20, pp. 6487–6495, 2008.

[29] K. Imai, S. Hirata, A. Irie et al., "Identification of HLA-A2-restricted CTL epitopes of a novel tumour-associated antigen, KIF20A, overexpressed in pancreatic cancer," *British Journal of Cancer*, vol. 104, no. 2, pp. 300–307, 2011.

[30] J. H. Sampson, A. B. Heimberger, G. E. Archer et al., "Immunologic escape after prolonged progression-free survival with epidermal growth factor receptor variant III peptide vaccination in patients with newly diagnosed glioblastoma," *Journal of Clinical Oncology*, vol. 28, no. 31, pp. 4722–4729, 2010.

Original Paper

Digestive Surgery

Dig Surg 2012;29:132–139
DOI: 10.1159/000337306

Received: October 19, 2011
Accepted after revision: February 13, 2012
Published online: April 24, 2012

Identification of the Lymphatic Drainage Pathways from the Pancreatic Head Guided by Indocyanine Green Fluorescence Imaging during Pancreaticoduodenectomy

Seiko Hirono Masaji Tani Manabu Kawai Ken-ichi Okada Motoki Miyazawa
Atsushi Shimizu Kazuhisa Uchiyama Hiroki Yamaue

Second Department of Surgery, Wakayama Medical University School of Medicine, Wakayama, Japan

Key Words
Lymphatic drainage pathway · Pancreatic head · Indocyanine green fluorescence imaging · Optimal lymphadectomy for pancreatic cancer

Abstract
Aims: We identified the lymphatic drainage pathways from the pancreatic head guided by indocyanine green (ICG) fluorescence imaging to analyze optimal lymphadectomy for pancreatic cancer. ***Methods:*** The lymphatic pathways in 20 patients undergoing pancreaticoduodenectomy were analyzed. We injected ICG into the parenchyma in the anterior (n = 10) or posterior surface (n = 10) of the pancreas head and observed the intraoperative lymphatic flows by ICG fluorescence imaging. ***Results:*** The seven main lymphatic drainage pathways were identified: (1) along the anterior or posterior pancreaticoduodenal arcade, (2) running obliquely down behind the superior mesenteric vein (SMV), (3) reaching the left side of the superior mesenteric artery (SMA), (4) running longitudinally upward between the SMV and SMA, (5) along the middle colic artery toward the transverse colon, (6) reaching the paraaortic (PA) region, and (7) reaching the hepatoduodenal ligament. The lymphatic pathway reaching the left side of the SMA was observed in 4 patients (20%), while that reaching the PA region in 17 patients (85%). The mean time to reach around the SMA was longer than that to reach the PA region. ***Conclusions:*** We found that several lymphatic drainage routes were observed from the pancreatic head, suggesting that a lymphadectomy around the SMA might have a similar oncological impact as that of the PA region.

Introduction

Pancreatic cancer generally has a poor prognosis because the incidence of invasion of extrapancreatic fatty tissue, including lymphatic vessels and nerves, and distant metastasis is high [1–3]. The only chance of cure for pancreatic cancer is surgical resection followed by adjuvant chemotherapy [4]; however, the 5-year survival rate of patients undergoing curative resection remains a mere 7–25% [1–3]. Especially lymph node metastasis is the most important prognostic factor in the patients after surgical resection of pancreatic cancer [5–8]. Therefore, many surgeons have tried to perform an extended lymphadectomy as one strategy for improving survival in the patients with pancreatic cancer [9–12], since Fort-

KARGER

Fax +41 61 306 12 34
E-Mail karger@karger.ch
www.karger.com

0253–4886/12/0292–0132$38.00/0

Accessible online at:
www.karger.com/dsu

Hiroki Yamaue, MD
Second Department of Surgery
Wakayama Medical University School of Medicine
811-1 Kimiidera, Wakayama 641-8510 (Japan)
Tel. +81 73 441 0613, E-Mail yamaue-h@wakayama-med.ac.jp

ner [13] initially proposed 'regional pancreatectomy as en-bloc resection for pancreatic cancer with the lymphatic vessels and great vessels' in 1973. However, four prospective, randomized controlled studies were performed to analyze the potential advantage or disadvantage of an extended lymphadectomy in the patients with pancreatic head cancer, and it was suggested that the extended procedure did not benefit the overall survival, and there might even be a trend towards increased morbidity, including diarrhea and delayed gastric emptying [14–17].

Several reports have emphasized the importance of lymphadectomy along the superior mesenteric artery (SMA), including the first, second, and third jejunal arteries (J1, J2, and J3 regions) for locoregional control and improvement of survival in the patients with pancreatic head cancer [18–21]. They reported that the tissue adherent to the SMA might cause local recurrence after surgery, because the tissue contained the lymphatic structures from the uncinate process of the pancreas [22, 23], therefore they concluded that the circumferential clearance of the SMA, including J1, J2, and J3 regions, was needed in pancreatic head cancer [18, 19]. In all studies comparing the standard pancreatoduodenectomy (PD) and PD with extended lymphadectomy, extended lymphadectomy was focused on paraaortic (PA) lymph node dissection, but not lymph node dissection around the SMA, therefore no evidence was observed regarding the significance of the circumferential clearance of the SMA in pancreatic cancer.

Recently, an instrument providing fluorescence imaging of lymphatic flow, the photodynamic eye (PDE; Hamamatsu Photonics, Hamamatsu, Japan) [24], has been used in experimental and preliminary clinical studies for breast cancer and gastrointestinal cancer [25–28]. The indocyanine green (ICG) reagent is a 776-Da disulfonated small molecule and ICG absorbs light in the near-infrared range, with the maximum at a wavelength of 800 nm, and also emits maximal fluorescence at a wavelength of 840 nm when it binds to plasma proteins [29–32]. ICG fluorescence imaging has been reported to make it easy to distinguish lymphatic vessels and lymph nodes containing ICG particles from the surrounding tissue [24–28]. The PDE system, guided by ICG, can visualize the lymphatic drainage flow in the operating room in a real-time fashion [24–28].

The purpose of our study was to verify that extended lymphadectomy does not provide any substantial benefit regarding the locoregional control of pancreatic cancer, by visualizing the lymphatic pathway from the pancreatic head, using ICG fluorescence imaging. We first tried to identify the lymphatic pathways from the pancreatic head, by this new method using the PDE system, to analyze optimal lymphadectomy including that around the SMA basis on the lymphatic flows.

Materials and Methods

Patients

Our series consisted of 20 consecutive patients prospectively recruited who met the eligibility criteria of undergoing conventional pancreaticoduodenectomy (PD), pylorus-preserving PD (PpPD) or pylorus-resecting PD (PrPD) between October 2008 and June 2009 at Wakayama Medical University Hospital (WMUH).

The eligibility criteria were: (1) the maximum tumor diameter was <3 cm and located in the head of the pancreas, because massive cancerous invasion or intense desmoplastic reaction causes obstruction of the lymphatic vessels, and the dye would then be unable to follow the normal lymphatic flow, and (2) the age of the patients was <80 years. None of the patients received either chemotherapy or irradiation preoperatively. The procedures for this study were approved by the ethics committee of WMUH (No. 600), and written informed consent was obtained from each of the patients before he/she was included in this study.

Optimal Dose of ICG

To determine the optimal dose of ICG, we did the following: 25 mg of ICG (Diagnogreen; Daiichi Pharmaceutical, Tokyo, Japan) was diluted in a total of 5 ml. At first, the ability to observe lymphatic drainage was examined at 0.1 ml in 4 patients, but it was difficult to find the lymphatic flows with PDE in 2 of these patients (50%). Next, we checked the lymphatic drainage using 0.2 ml, and found that we could clearly observe the lymphatic flows that received ICG with PDF in all 4 patients (100%). Finally the ability to observe lymphatic drainage was examined at 0.4 ml. However, at this level, we could not distinguish lymphatic vessels from the surrounding adipose tissue, because ICG spread diffusely and was visualized as large shining fluorescent spots with PDE in 3 of the 4 patients (75%). On the basis of these results, we decided to inject 0.2 ml throughout the subsequent experiments using the 20 enrolled patients. Injection into the parenchyma in the anterior or posterior surface was alternately selected in the enrolled patients.

Technique

After laparotomy, Kocher's maneuver was performed carefully, and then gastric or duodenal resection was performed. A 0.2-ml aliquot of 0.5% ICG solution was injected into the parenchyma in the anterior or posterior surface of the uncinate process of the pancreas with a 26-gauge needle at a depth of 0.5 mm.

We observed intraoperative lymphatic drainage flows from the uncinate process of the pancreas by ICG fluorescence imaging using the PDE system. The fluorescence signals were transmitted to a digital video processor to be displayed on a TV monitor in real time. We assessed the pattern of spread of the ICG by the PDE for the initial 15 min after ICG injection, and also observed the

Table 1. Clinicopathological characteristics of the patients injected with ICG

No.	Age	Sex	Final histopathological diagnosis	Tumor size, cm	Operation	TNM stage[1]	Perineural invasion	Ratio of N+/N–
Patients injected with ICG into the anterior surface of the uncinate pancreas								
1	62	M	distal bile duct cancer	2.5	PrPD	T3, N1, M0; stage IIB	positive	2/11
2	77	F	distal bile duct cancer	1.2	PpPD	T3, N1, M0; stage IIB	positive	7/17
3	63	M	distal bile duct cancer	1.4	PrPD	T3, N0, M0; stage IIA	negative	0/13
4	69	M	pancreatic ductal adenocarcinoma	2.9	PrPD	T3, N1, M0; stage IIB	negative	2/13
5	70	F	pancreatic ductal adenocarcinoma	2.2	PrPD + SMV resection	T3, N1, M0; stage IIB	negative	1/33
6	61	F	pancreatic ductal adenocarcinoma	1.0	PrPD	T1, N0, M0; stage IA	negative	0/10
7	72	M	pancreatic ductal adenocarcinoma	2.8	PrPD + SMV resection	T3, N1, M0; stage IIB	negative	2/22
8	75	M	distal bile duct cancer	1.5	PpPD	T1, N1, M0; stage IIB	negative	4/21
9	58	F	chronic pancreatitis (tumor forming)	2.0	PrPD	–	–	–
10	67	F	pancreatic ductal adenocarcinoma	2.0	PD	T3, N0, M0; stage IIA	negative	0/11
Patients injected with ICG into the posterior surface of the uncinate pancreas								
11	69	F	pancreatic ductal adenocarcinoma	1.5	PpPD	T1, N0, M0; stage IA	negative	0/36
12	68	M	pancreatic ductal adenocarcinoma	2.3	PrPD	T3, N1, M0; stage IIB	negative	3/11
13	60	M	pancreatic ductal adenocarcinoma	1.8	PrPD	T3, N0, M0; stage IIA	negative	1/19
14	75	M	distal bile duct cancer	1.4	PrPD	T3, N1, M0; stage IIB	positive	1/29
15	65	F	pancreatic ductal adenocarcinoma	1.5	PpPD	T3, N0, M0; stage IIA	negative	0/14
16	75	F	pancreatic ductal adenocarcinoma	2.3	PrPD + SMV resection	T3, N1, M0; stage IIB	negative	2/27
17	71	M	pancreatic ductal adenocarcinoma	1.6	PrPD	T1, N1, M0; stage IIB	negative	2/15
18	79	F	distal bile duct cancer	1.3	PrPD	T3, N0, M0; stage IIA	negative	0/12
19	64	F	pancreatic ductal adenocarcinoma	1.0	PrPD	T1, N0, M0; stage IA	negative	0/12
20	53	M	pancreatic ductal adenocarcinoma	2.5	PrPD + SMV resection	T3, N1, M0; stage IIB	negative	4/45

[1] TNM classification of the Union internationale contre le cancer.

lymphatic flow at the time of resection of the bile duct (mean 50 min, range 29–110) and resection of the pancreas (mean 87 min, range 57–137). We performed sampling or dissection en bloc of tissue received ICG and then diagnosed these tissues in pathological examination.

Results

Patient Characteristics

Table 1 shows the clinicopathological characteristics of the patients in this study. The patients included 10 males and 10 females, with an average age of 68.2 ± 6.7 years (range 53–79). The final pathological diagnosis showed that 13 patients had pancreatic ductal adenocarcinoma, 6 had distal bile duct cancer, and 1 had tumor-forming pancreatitis. The mean size of the pancreatic tumors was 1.9 ± 0.6 cm (range 1.0–2.9). According to the UICC TNM classification [33], among 13 patients with pancreatic ductal carcinoma, 3 patients were stage IA, 3 patients were IIA, and 7 patients were stage IIB, while among the 6 patients with bile duct cancer, 2 patients were stage IIA and 4 patients were stage IIB. According to pathological examinations, 3 patients (15.8%) had perineural invasion and 10 patients (52.6%) had lymph node metastasis. 15 patients underwent PrPD, 4 PpPD, and 1 PD, and 4 patients also underwent a combined the superior mesenteric vein (SMV) resection.

Lymphatic Pathways from the Uncinate Process of the Pancreas and the Mean Time to Arrive at the Drainage Areas

There were no patients with complications or adverse events related to intraoperative injection of ICG, regardless of the dose (up to 0.4 ml). Immediately after the ICG injection, we were able to locate the lymphatic vessels draining the uncinate process of the pancreas as shining fluorescent streams and spots in fluorescence images of the PDE, whereas no lymphatic flow was clearly visible as green in color after ICG injection, and could not be easily judged as being lymphatic vessels by naked-eye examination.

The lymphatic drainage routes from the uncinate process of the pancreas detected with PDE are shown in tables 2 and 3. Seven main lymphatic pathways from the

Table 2. Lymphatic drainage pathways in the patients injected with ICG into the anterior surface of the uncinate process of the pancreas

No.	Anterior pancreaticoduodenal arcade	Behind the SMV	Left side of the SMA (J1, J2, J3 regions)	Longitudinally upward between the SMV and SMA	Origin of the middle colonic artery toward the transverse colon	PA region	Hepatoduodenal ligament
1	○	○	○	○	○	○	×
2	○	○	○	○	○	○	×
3	○	○	○	×	○	○	×
4	○	○	×	○	○	○	×
5	○	○	○	×	○	○	×
6	○	○	×	×	○	○	×
7	○	○	×	×	○	○	×
8	○	○	×	○	○	×	×
9	○	○	×	×	×	○	×
10	○	○	×	×	○	×	×

Table 3. Lymphatic drainage pathways in the patients injected with ICG into the posterior surface of the uncinate process of the pancreas

No.	Posterior pancreaticoduodenal arcade	Behind the SMV	Left side of the SMA (J1, J2, J3 regions)	Longitudinally upward between the SMV and SMA	Origin of the middle colonic artery toward the transverse colon	PA region	Hepatoduodenal ligament
11	○	○	×	○	○	○	×
12	○	○	×	×	○	○	×
13	○	○	×	○	×	○	○
14	○	○	×	○	○	○	×
15	○	○	×	○	×	○	○
16	○	○	×	○	×	○	×
17	○	○	×	×	×	○	○
18	○	×	×	×	×	○	×
19	○	×	×	×	×	○	×
20	○	×	×	×	×	×	×

uncinate process of the pancreas were observed with PDE. The lymphatic pathways were observed (1) along the anterior or posterior pancreaticoduodenal arcade, (2) running obliquely down behind the SMV, (3) passing behind the SMV and SMA and reaching the left side of the SMA (J1, J2, or J3 regions), (4) passing behind the SMV and running longitudinally upward between the SMV and SMA, (5) passing the origin of the middle colonic artery toward the transverse colon, (6) reaching the PA region, and (7) reaching the hepatoduodenal ligament.

Table 2 shows the lymphatic drainage pathways in the patients with injection of ICG into the anterior surface of the uncinate process of the pancreas (n = 10). We could identify the lymphatic flow along the anterior pancreaticoduodenal arcade in all 10 patients (100%) within 5 min after ICG injection. The lymphatic flow running obliquely down and shining fluorescent spots behind the SMV were found in all 10 patients (100%) with an ICG injection into the anterior surface, and then the lymphatic flow reaching on the left side of the SMA (J1, J2, or J3 region) was observed in 4 patients (40%). We observed the lymphatic flow running longitudinally upward between the SMV and SMA from the anterior surface in 4 patients (40%). Shining at the origin of the middle colonic artery was observed in 9 patients (90%) with the anterior injection. The lymphatic flow reaching the PA region was found in 8 patients (80%) who receive an ICG injection into the anterior surface, whereas the lymphatic flow reaching the hepatoduodenal ligament was not found in any patients with the anterior injection.

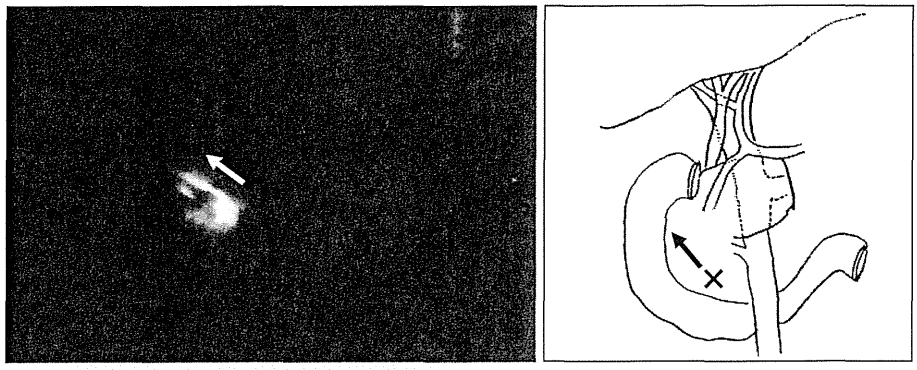

Fig. 1. Lymphatic flow from the anterior surface of the uncinate process of the pancreas toward the duodenal wall and then spread along the anterior pancreaticoduodenal arcade. × = Injection site, the arrow indicates the lymphatic flow visualized by the ICG fluorescence imaging system.

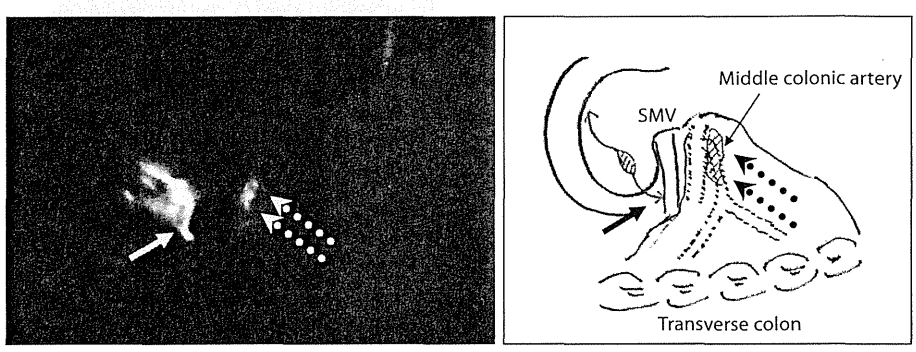

Fig. 2. Lymphatic flow running obliquely down behind the SMV was observed (a solid arrow), and at the same time, a shining spot at the origin of the middle colonic artery was observed (dotted arrows) in the patient who received an anterior injection.

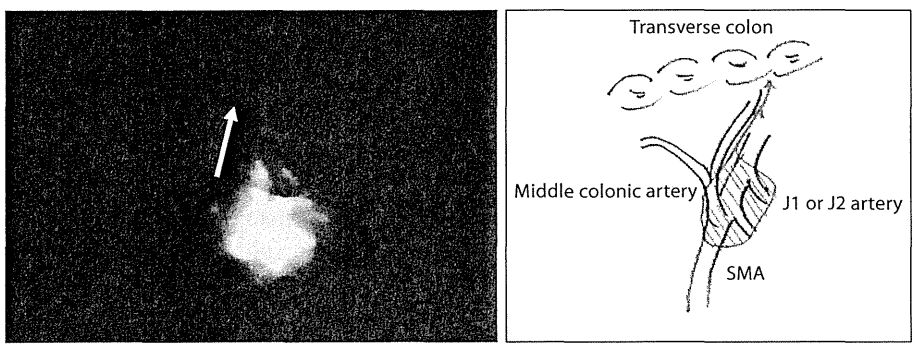

Fig. 3. Shining spots on the left side area of the SMA (J1 or J2) were observed in the patient who received an anterior injection. The lymphatic flow moving to the transverse colon through the middle colonic artery was observed.

Table 3 shows the lymphatic drainage pathways in the patients with an ICG injection into the posterior surface of the uncinate process (n = 10). We observed the lymphatic flow along the posterior pancreaticoduodenal arcade in all 10 patients (100%) immediately after ICG injection into the posterior surface. The lymphatic flow running obliquely down behind the SMV from the posterior surface of the uncinate process was found in 7 patients (70%), but reaching on the left side of the SMA was not observed in any patients with an ICG injection into the posterior surface. The lymphatic flow running longitudinally upward between the SMV and SMA from the posterior surface was observed in 5 patients (50%), and the lymphatic flow passing the origin of the middle colonic artery toward the transverse colon was observed in 3 patients (30%) with the posterior injection. The lymphatic flow reaching the PA region was found in 9 patients (90%) who received an ICG injection into the posterior surface, and the lymphatic flows reaching the hepatoduodenal ligament in 3 patients (30%).

Figure 1 shows the lymphatic flow toward the duodenal wall and then along the anterior pancreaticoduodenal arcade in case 1, with the injection of ICG at the anterior surface of the pancreas head. Figure 2 shows the lymphatic flow running obliquely down behind the SMV, and at the same time, the shining spot at the origin of the middle colonic artery, when ICG was injected in the anterior surface (case 1). Figure 3 shows the shining spots on the left side of the SMA (J1 and J2 regions), and the lymphatic flow passing the origin of the middle colic ar-

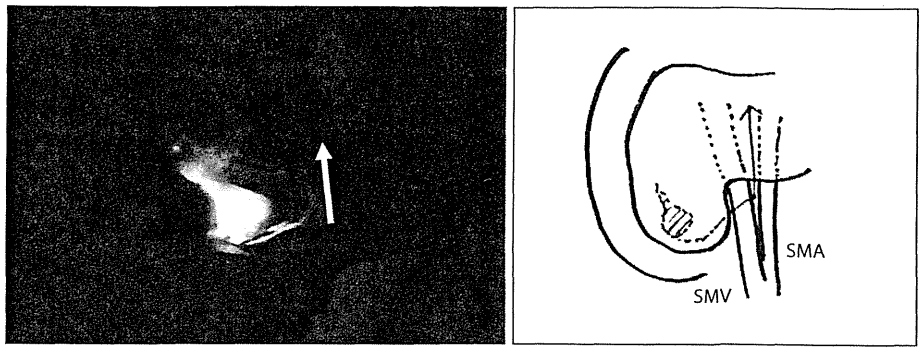

Fig. 4. Lymphatic flow running longitudinally upward between the SMV and SMA was observed in the patient who received a posterior injection.

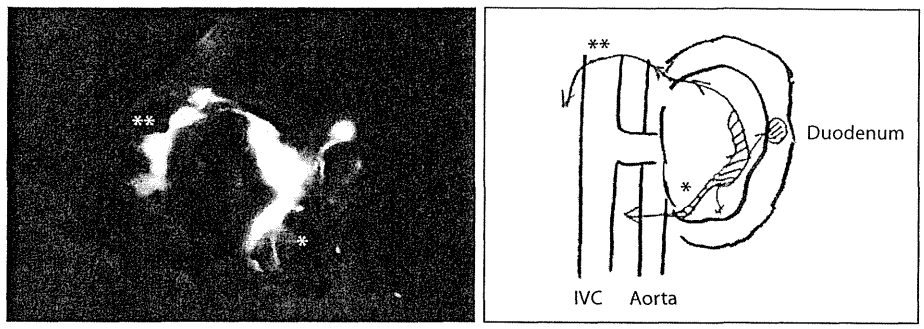

Fig. 5. Shining spots in the PA area were observed. There were two routes toward the PA area; one was the flow directly from the posterior pancreatic head (*), and the other was the flow passing the origin of the SMA toward the anterior inferior vena cava (**).

Table 4. Mean time to arrival at the shining spots from the uncinate process of the pancreas

Injection	Anterior or posterior pancreaticoduodenal arcade	Behind the SMV	Left side of the SMA (J1, J2, J3 regions)	Longitudinally upward between the SMV and SMA	Origin of the middle colonic artery toward the transverse colon	PA region	Hepatoduodenal ligament
Anterior surface of the uncinate process	2.0 min (0.5–4.5)	10.7 min (5–30)	41.8 min (7–80)	21.3 min (10–30)	8.4 min (1–30)	8.2 min (1–30)	–
Posterior surface of the uncinate process	1.6 min (0.5–4)	50.3 min (5–80)	–	38.2 min (5–78)	35.0 min (25–50)	7.2 min (1–50)	38 min (4–60)

Values in parentheses show the range of time to arrive after ICG injection.

tery toward the transverse colon in case 1, with the anterior injection. Figure 4 shows the lymphatic flow running longitudinally upward between the SMV and SMA when ICG was injected into the posterior surface (case 14). Figure 5 shows the lymphatic pathways reaching the PA regions from the anterior surface of the uncinate process (case 1). There were two routes that were observed to shine in the PA area; one was the lymphatic flow directly to the PA area from the posterior surface of the pancreas, and the other was the lymphatic flow passing the origin of the SMA toward the PA area, and then passing the anterior inferior vena cava and reaching the right side of the inferior vena cava.

The mean time to arrive at the each of the shining spots after ICG injection is shown in table 4. The mean arrival time of the drainage pathway reaching around the SMA was longer than that reaching the PA region following both the anterior and posterior injections (21.3 min, 38.2 vs. 8.1 min, 7.2 min).

Histopathological Examination of Tissues That Received ICG

We performed sampling of the PA tissue received in 11 of the 13 patients with pancreatic cancer who were found to have lymphatic flow to the PA tissue. None of the sampled tissue specimens contained malignant deposits on final histopathological examination. In only 1 patient with pancreatic cancer in whom we had observed shining in the left side of the SMA, we dissected en bloc the left side region of the SMA, and no malignant cells around the SMA were found in pathological examination.

Discussion

Several studies have tried to identify the lymphatic pathways in pancreatic cancer patients to determine the optimal lymphadectomy procedure, however the pattern of lymphatic drainage and draining areas remained poorly defined [22–35]. Deki and Sato [22] reported the lymphatic pathways of the pancreas by dissecting the lymphatic vessels using a cadaver. This report described that the lymphatic vessels running obliquely down and passing behind the SMA and SMV and linking with lymph nodes located between these vessels and the posterior layer of the mesentery were observed in the anterior pancreatic head. It has also been reported using autopsy specimens that the lymphatic pathway from the posterior pancreatic head drains toward the right or posterior side of the SMA and finally to the PA lymph nodes [23]. Although these studies did provide useful information, as they used only autopsy specimens, they could not identify the physiological lymphatic flow from the pancreas in a real-time fashion. In another study, sentinel lymph node mapping of pancreatic head cancer was studied by methylene blue dye injection, however the study failed and concluded that it was not possible to identify lymphatic drainage from the pancreatic head using their technology [34].

In this study, we injected ICG into the anterior or posterior surface of the uncinate process of the pancreas, after determining the optimal concentration of ICG by examining various concentrations [28], and then evaluated the time to arrive at the lymphatic drainage areas. The reasons that we chose the uncinate process as injected location of ICG are (1) cancer in the ventral pancreatic head occurs more often than that in the dorsal pancreatic head [20], and (2) it has been reported that lymph node metastasis around the SMA is most often in the cancer located in the uncinate process [18, 19].

We could identify the visual lymphatic drainage pathways from the head of the pancreas by ICG fluorescence imaging during surgery. Indeed, we found the lymphatic root passing behind the SMV and SMA around the left side of the SMA from the anterior pancreatic head, as the previous anatomic reports description, however we also simultaneously found several other roots including the PA region. With regard to the relationship between lymphatic drainage and the clinical significance of lymph node metastasis, of the 16 patients demonstrating lymphatic drainage to the PA region, 6 patients had no lymph node metastasis and 10 patients had lymph node metastasis in only the regional lymph node. As a result, we did not find any relationship between lymphatic drainage and the clinical outcome.

This study showed that (1) the lymphatic drainage to the PA region from the pancreatic head was more often than that to the left side of the SMA (J1, J2, and J3 regions), (2) the patients with lymphatic drainage into the left side of the SMA have a simultaneous pathway into the PA region, and (3) the time reaching around the SMA was longer than that reaching the PA region. Based on these results, a lymphadenectomy of the left side of the SMA, including the J1, J2, and J3 regions, might have a similar oncological impact as a lymphadenectomy around the PA region, that is, the circumferential clearance of the SMA may not be of benefit as PA lymph node dissection is for patients with pancreatic cancer, although prospective randomized controlled studies would be needed to prove our conclusion.

References

1 Michalski CW, Kleef J, Wente MN, et al: Systematic review and meta-analysis of standard and extended lymphadenectomy in pancreaticoduodenectomy for pancreatic cancer. Br J Surg 2007;94:265–273.
2 Pawlik TM, Abdalla EK, Barnett CC, et al: Feasibility of a randomized trial of extended lymphadectomy for pancreatic cancer. Arch Surg 2005;140:584–591.
3 Alexakis N, Halloran C, Raraty M, et al: Current standards of surgery for pancreatic cancer. Br J Surg 2004;91:1410–1427.
4 Stocken DD, Büchler MW, Dervenis C, et al: Meta-analysis of randomized adjuvant therapy trials for pancreatic cancer. Br J Cancer 2005;92:1372–1381.
5 Hirono S, Yamaue H, Hoshikawa Y, et al: Molecular markers associated with lymph node metastasis inn pancreatic ductal adenocarcinoma by genome-wide expression profiling. Cancer Sci 2010;101:259–266.

6 Riediger H, Keck T, Wellner U, et al: The lymph node ratio is the strongest prognostic factor after resection of pancreatic cancer. J Gastrointest Surg 2009;13:1337–1344.
7 Zacharias T, Jaeck D, Neuville OA, et al: Impact of lymph node involvement on long-term survival after R0 pancreaticoduodenectomy for ductal adenocarcinoma of the pancreas. J Gastrointest Surg 2007;11:350–356.
8 Nakao A, Harada A, Nonami T, et al: Lymph node metastases in carcinoma of the head of the pancreas region. Br J Surg 1995;82:399–402.
9 Ishikawa O, Ohhigashi H, Sasaki Y, et al: Practical usefulness of lymphatic and connective tissue clearance for the carcinoma of the pancreas head. Ann Surg 1988;208:215–220.
10 Manabe T, Ohshio G, Baba N, et al: Radical pancreatectomy for ductal cell carcinoma of the head of the pancreas. Cancer 1989;64:1132–1137.
11 Nakao A, Takeda S, Inoue S, et al: Indications and techniques of extended resection for pancreatic cancer. World J Surg 2006;30:976–982.
12 Kato K, Yamada S, Sugimoto H, et al: Prognostic factors for survival after extended pancreatectomy for pancreatic head cancer. Influence of resection margin status on survival. Pancreas 2009;38:605–612.
13 Fortner JG: Regional resection and pancreatic carcinoma. Surgery 1973;73:799–800.
14 Pedrazzoli S, DiCarlo V, Dionigi R, et al: Standard versus extended lymphadenectomy associated with pancreatoduodenectomy in the surgical treatment of adenocarcinoma of the head of the pancreas: a multicenter, prospective, randomized study. Lymphadenectomy Study Group. Ann Surg 1998;228:508–517.
15 Yeo CJ, Cameron JL, Lillemoe KD, et al: Pancreaticoduodenectomy with or without distal gastrectomy and extended retroperitoneal lymphadectomy for periampullary adenocarcinoma. Part 2. Randomized controlled trial evaluating survival, morbidity and mortality. Ann Surg 2002;236:355–366.
16 Farnell MB, Pearson RK, Sarr MG, et al: A prospective randomized trial comparing standard pancreatoduodenectomy with extended lymphadectomy in resectable pancreatic head adenocarcinoma. Surgery 2005;138:618–628.
17 Nimura Y, Nagino M, Kato H, et al: Regional versus extended lymph node dissection in radical pancreaticoduodenectomy for pancreatic cancer: a multicenter, randomized controlled trial (abstract). HPB 2004;6(suppl 1):2.
18 Kayahara M, Nagakawa T, Kobayashi H, et al: Lymphatic flow in carcinoma of the head of the pancreas. Cancer 1992;70:2061–2066.
19 Kayahara M, Nagakawa T, Kobayashi K, et al: Analysis of paraaortic lymph node involvement in pancreatic carcinoma: a significant indication for surgery? Cancer 1999;85:583–590.
20 Kitagawa H, Ohta T, Tani T, et al: Carcinoma of the ventral and dorsal pancreas exhibit different patterns of lymphatic spread. Front Biosci 2008;13:2728–2735.
21 Pessaux P, Varma D, Arnaud FP: Pancreaticoduodenectomy: superior mesenteric artery first approach. J Gastrointest Surg: 2006;10:607–611.
22 Deki H, Sato T: An anatomic of the peripancreatic lymphatics. Surg Radiol Anat 1998;10:121–135.
23 Nagai H, Kuroda A, Morioka Y: Lymphatic and local spread of T1 and T2 pancreatic cancer. Ann Surg 1986;204:65–71.
24 Kitai T, Inomoto T, Miwa M, et al: Fluorescence navigation with indocyanine green for detecting sentinel lymph nodes in breast cancer. Breast Cancer 2005;12:211–215.
25 Ogasawara Y, Ikeda H, Takahashi M, et al: Evaluation of breast lymphatic pathways with indocyanine green fluorescence imaging in patients with breast cancer. World J Surg 2008;32:1924–1929.
26 Tajima Y, Yamazaki K, Masuda Y, et al: Sentinel node mapping guided by indocyanine green fluorescence imaging in gastric cancer. Ann Surg 2009;249:58–62.
27 Kusano M, Tajima Y, Yamazaki K, et al: Sentinel node mapping guided by indocyanine green fluorescence imaging: a new method for sentinel node navigation surgery in gastrointestinal cancer. Dig Surg 2008;25:103–108.
28 Noura S, Ohue M, Seki Y, et al: Feasibility of a lateral region sentinel node biopsy of lower rectal cancer guided by indocyanine green using a near-infrared camera system. Ann Surg Oncol 2010;17:144–151.
29 Caesar J, Shaldon S, Chiandussi L, et al: The use of indocyanine green in the measurement of hepatic blood flow and as a test of hepatic function. Clin Sci 1961;21:43–57.
30 Cherrick GR, Stein SW, Leevy CM, et al: Indocyanine green: observations on its physical properties, plasma decay, and hepatic extraction. J Clin Invest 1960;39:592–600.
31 Nimura H, Narimiya N, Mitsumori M, et al: Infrared ray electronic endoscopy combined with indocyanine green injection for detection of sentinel nodes of patients with gastric cancer. Br J Surg 2004;91:575–579.
32 Ishikawa K, Yasuda K, Shiromizu A, et al: Laparoscopic sentinel node navigation achieved by infrared ray electronic endoscopy system in patients with gastric cancer. Surg Endosc 2007;21:1131–1134.
33 Sobin LH, Wittekind C: International Union Against Cancer. TNM Classification of Malignant Tumor, ed 6. New York, Wiley-Liss, 2002.
34 Kocher HM, Sohail M, Benjamin IS, et al: Technical limitations of lymph node mapping in pancreatic cancer. Eur J Surg Oncol 2007;33:887–891.
35 Evans BP, Ochsner A: The gross anatomy of the lymphatics of the human pancreas. Surgery 1954;36:177–191.

The Carcinoembryonic Antigen Level in Pancreatic Juice and Mural Nodule Size Are Predictors of Malignancy for Branch Duct Type Intraductal Papillary Mucinous Neoplasms of the Pancreas

Seiko Hirono, MD, Masaji Tani, MD, Manabu Kawai, MD, Ken-ichi Okada, MD, Motoki Miyazawa, MD, Atsushi Shimizu, MD, Yuji Kitahata, MD, and Hiroki Yamaue, MD

Objective: Identification of predictors of malignancy for branch duct type intraductal papillary mucinous neoplasms (IPMN).

Background: Main duct type IPMN has been recommended for resection. However, the indications for resection of the branch duct type IPMN have been controversial.

Methods: We retrospectively analyzed the clinicopathological factors of 134 patients undergoing resection for branch duct type IPMN, excluding main duct type IPMN, to identify predictors of the malignant behavior of this neoplasm. The cutoff values of tumor size, main pancreatic duct (MPD) size, mural nodule size, and carcinoembryonic antigen (CEA) level in the pancreatic juice obtained during preoperative endoscopic retrograde pancreatography (ERP) were analyzed using receiver–operator characteristic curves.

Results: We found 7 significant predictors for malignancy in the branch duct type IPMN in a univariate analysis; jaundice, tumor occupying the pancreatic head, MPD size >5 mm, mural nodule size >5 mm, serum carbohydrate antigen (CA)19–9 level, positive cytology in the pancreatic juice, and CEA level in the pancreatic juice >30 ng/mL. In a multivariate analysis, a mural nodule size >5 mm and a CEA level in the pancreatic juice >30 ng/mL were independent factors associated with malignancy. The positive predictive value of a mural nodule size >5 mm and a CEA level in the pancreatic juice >30 ng/mL was 100%, and the negative predictive value was 96.3%.

Conclusions: We identified 2 useful predictive factors for malignancy in branch duct type IPMN; a mural nodule size >5 mm and a CEA level in the pancreatic juice obtained by preoperative ERP >30 ng/mL.

(*Ann Surg* 2012;255:517–522)

As a result of improvements of radiological imaging and increased clinician awareness, intraductal papillary mucinous neoplasm (IPMN) of the pancreas has been recognized with increasing frequency because it was formally defined in 1996 by the World Health Organization.[1] It has been established that IPMN has malignant potential and that it first transforms from an adenoma to a borderline neoplasm, then develops into carcinoma, including carcinoma in situ (CIS), and ultimately becomes an invasive carcinoma [invasive IPMC (intraductal papillary mucinous carcinoma)].[1] In general, IPMN has a favorable prognosis, because of its indolent biological behavior; therefore, excellent survival outcomes have been reported after complete resection in the patients with noninvasive IPMN, including adenoma, borderline neoplasm, and CIS.[2–6] However, once IPMN progresses to invasive carcinoma, it becomes aggressive and is associated with a poor prognosis, with the 5-year survival in patients with invasive IPMC reportedly ranging from 22% to 67%.[7–9] Therefore, the timing of resection is important for the successful treatment of IPMN, and it is necessary to establish a treatment protocol and surgical indications for patients with IPMN.

Depending on the morphology of the changes of the ductal system, IPMNs have been classified into the 3 variations—main duct type, branch duct type, and mixed type by radiological imaging. Many recent clinicopathological studies have shown that IPMNs arising in the main pancreatic duct (MPD) are more aggressive than those arising in the branch pancreatic duct (BPD), and the malignancy rate of main duct type IPMN has been reported to be 57% to 92%,[4–6,10] whereas that of branch duct type IPMN has been reported to be 6% to 58%.[10–14] Therefore, although most clinicians agree that surgical resection is required for all main duct type IPMNs, the management of branch duct type IPMNs remains controversial, because branch duct type IPMN generally has a low risk of malignancy.

We previously suggested that measurement of the carcinoembryonic antigen (CEA) level in the pancreatic juice obtained during preoperative endoscopic retrograde pancreatography (ERP) was useful for distinguishing malignant from benign IPMNs,[2,3]; however, our previous studies had 2 problems: (1) a small number of patients analyzed (n = 54), and (2) the subjects in the study were patients with all types of IPMNs, including the main duct type. Therefore, in the present study, we examined 134 patients with IPMNs, other than the main duct type, and reanalyzed the cutoff values for predicting malignancy of the tumor size, MPD size, mural nodule size, and the CEA level in the pancreatic juice, using receiver–operator characteristic (ROC) curves. We retrospectively analyzed the clinical and imaging findings and laboratory data to identify the predictors of malignancy and determined the optimal indications for the patients with branch duct type IPMN.

MATERIALS AND METHODS

Patient Enrollment

From July 1999 to February 2011, 196 consecutive patients with IPMN underwent a pancreatectomy at Wakayama Medical University Hospital. We classified the patients into 2 groups on the basis of their type of IPMN as determined by preoperative imaging studies; main duct type IPMN and branch duct type IPMN. We defined the main duct type IPMN as that found to have diffuse or segmental MPD dilation, but not cyst formation caused by BPD dilation. Next, we defined the branch duct type IPMN as that with cyst formation caused by BPD dilation with or without MPD dilation. In this study, we excluded 23 patients who had IPMN concomitant with common pancreatic cancer. Among the remaining 173 consecutive patients with resected IPMNs, 134 patients were classified as having branch duct type IPMN, and all were enrolled in this study. The study protocol was approved by the Human Ethics Review Committee of Wakayama Medical University Hospital, and a signed consent form was obtained from each subject.

From the Second Department of Surgery, Wakayama Medical University, School of Medicine, Kimiidera, Wakayama, Japan.

Disclosure: The authors declare that they have nothing to disclose.

Reprints: Hiroki Yamaue, MD, Second Department of Surgery, Wakayama Medical, University, School of Medicine, 811–1 Kimiidera, Wakayama 641–8510, Japan. E-mail: yamaue-h@wakayama-med.ac.jp.

ISSN: 0003-4932/12/25503-0517
DOI: 10.1097/SLA.0b013e3182444231

Preoperative Examination and Indications for Surgery

Before surgery, all patients underwent a clinical evaluation, routine laboratory tests including the assessment of tumor markers, abdominal ultrasonography (US), and computed tomography (CT). Magnetic resonance imaging cholangiopancreatography and endoscopic US (EUS) were performed in 131 and 125 patients, respectively. Endoscopic retrograde pancreatography was performed in all patients with branch duct type IPMN, excluding the 4 patients undergoing Billroth II reconstruction after distal gastrectomy. Preoperative pancreatic juice cytology (n = 104) and measurement of CEA levels in pancreatic juice (n = 91) were performed using the samples obtained during preoperative ERP, using the previously reported method.[2,3] Briefly, the pancreatic juice in the MPD was collected by preoperative ERP, and immediately centrifuged, and the precipitate was used for cytological examination, and the CEA levels in the supernatant were measured by means of a CEA immunometric chemiluminescent assay kit (Bayer Medical Co, Tokyo, Japan). The tumor size was measured by CT, and the mural nodule size was determined by EUS in 125 patients who underwent preoperative EUS, and by CT in other 9 patients without performing EUS.

Surgery was performed in the patients with IPMN who met at least one of the following criteria: (1) the presence of symptoms, (2) main duct type IPMN, (3) the presence of mural nodules, (4) an MPD larger than 7 mm in diameter, or gradual dilation of the MPD observed during follow-up, (5) tumor size larger than 30 mm, or a gradual increase in the tumor size during follow-up, (6) class IV or V in cytology of the pancreatic juice, or (7) a CEA level higher than 110 ng/mL in the pancreatic juice, which was the cutoff level identified by analyzing the difference between benign and malignant IPMNs in all patients with all types of IPMN, using ROC curves, as previously reported.[2,3]

All resected specimens were examined pathologically and classified into adenoma, borderline, CIS, and invasive IPMC, according to the classification established by the World Health Organization by 2 independent pathologists (A.Y. and Y.N.). *Invasive IPMC* was defined as that presenting the pathological findings of continuance of an invasive component from CIS, to distinguish it from common pancreatic ductal cancer concomitant with IPMN.

Statistical Analysis

For the purpose of the analyses, we classified IPMN with adenoma and borderline neoplasm as a benign IPMN group, whereas CIS and invasive IPMC were classified as a malignant IPMN group. The cutoff levels for the tumor size, MPD size, mural nodule size, and CEA level in the pancreatic juice were determined to maximize the difference between benign and malignant IPMNs by ROC curves (SPSS, Release 17.0; SPSS Inc, Chicago, IL). The 16 preoperative potential risk factors were assessed by a univariate analysis with the χ^2 and included the patient age, sex, symptoms, jaundice, body weight loss, abdominal pain, back pain, diabetes mellitus, the tumor location, tumor size, MPD size, mural nodule size, serum CEA level, serum carbohydrate antigen (CA) 19–9 level, cytology in the pancreatic juice, and CEA levels in the pancreatic juice (SPSS, Release 17.0). The $P < 0.1$ predictors of malignant IPMN in the univariate analysis were then included in a forward stepwise multiple logistic regression model (SPSS, Release 17.0). Statistical significance was defined as $P < 0.05$.

RESULTS

Patient Characteristics and Histopathological Findings

Table 1 shows the characteristics of the enrolled patients. This study included 74 men and 60 women, with a mean age ± standard deviation of 68.9 ± 9.7 years. The mean tumor size, mean MPD size, and the mean mural nodule size were 30.4 ± 12.3, 6.5 ± 4.2, and 5.5 ± 5.0, respectively. A total pancreatectomy was performed in 3 patients (2.2%); a pancreatoduodenectomy (PD), including a pylorus-preserving PD and a pylorus-resecting PD, was performed in 101 patients (75.4%); a distal pancreatectomy was performed in 14 patients (10.5%); and a central pancreatectomy was performed in 16 patients (11.9%). Combined venous resection (portal vein or superior mesenteric vein) was performed in 10 patients (7.4%), and combined celiac artery resection was performed in 1 patient (0.8%).

In the 134 patients with branch duct type IPMN, there were 56 patients (41.8%) with benign IPMN, including 51 with adenomas and 5 with borderline neoplasms, and there were 41 patients (30.6%) with CIS, and 37 patients (27.6%) with invasive IPMC, including 5 with minimally invasive IPMC (Table 1).

Complications of ERP and Pancreatic Duct Irrigation

The definition of post-ERP acute pancreatitis and the grading of its severity were based on consensus criteria.[15] Seven patients (5.4%) developed pancreatitis in 130 patients who underwent preoperative ERP. Among them, 5 patients (4.8%) developed pancreatitis (moderate in 1 patient and mild in 4 patients) in 104 patients whose pancreatic juice obtained by ERP.

Diagnostic Cutoff Levels for the Tumor Size, MPD Size, Mural Nodule Size, and CEA Levels in the Pancreatic Juice for the Prediction of Malignant IPMN

In this study, ROC curves were used to determine the cutoff levels for the tumor size, MPD size, mural nodule size, and CEA level in the pancreatic juice (Fig. 1) to differentiate between benign and malignant IPMN in the patients with the branch duct type IPMN. Mathematically, the cutoff values were defined as those corresponding to points on the ROC curve situated furthest away from the reference line. The areas under curve for the tumor size, MPD size, mural nodule size, and CEA level in the pancreatic juice were 0.612, 0.711, 0.819, and 0.920, respectively, and the determined cutoff levels for the differentiation between benign and malignant IPMNs were 30 mm, 5 mm, 5 mm, and 30 ng/mL, respectively (Table 2).

TABLE 1. The Demographics and Clinical Characteristics of 134 Patients With Branch Duct Type IPMN

Characteristics	Value
Age, mean ± SD (range), yr	68.9 ± 9.7 (32–84)
Sex, male/female	74/60
Tumor size, mean ± SD (range), mm	30.4 ± 12.3 (5–88)
Main pancreatic duct size, mean ± SD (range), mm	6.5 ± 4.2 (1–20)
Mural nodule size, mean ± SD (range), mm	5.5 ± 5.0 (0–20)
Operation	
Total pancreatectomy	3 (2.2%)
Pancreatoduodenectomy (PD/PpPD/PrPD)	101(17/43/41) (75.4%)
Distal pancreatectomy	14 (10.5%)
Central pancreatectomy	16 (11.9%)
Histopathology	
Adenoma	51 (38.1%)
Borderline	5 (3.7%)
Carcinoma in situ	41 (30.6%)
Invasive IPMC	37 (27.6%)

PpPD indicates pylorus-preserving PD; PrPD, pylorus-resecting PD

Predictors of Malignancy for Branch Duct Type IPMN

In the univariate analysis, we found 7 significant factors predicting the malignancy of branch duct type IPMNs: the presence of jaundice ($P < 0.001$), a tumor occupying the pancreatic head ($P = 0.006$), a MPD size larger than 5 mm ($P < 0.001$), mural nodule size larger than 5 mm ($P < 0.001$), elevated serum CA19–9 ($P = 0.002$), positive cytology (class IV or V) in the pancreatic juice ($P = 0.023$), and a CEA level in the pancreatic juice >30 ng/mL ($P < 0.001$) (Table 3). Furthermore, a mural nodule size larger than 5 mm ($P = 0.003$; odds ratio = 12.9) and a CEA level in the pancreatic juice higher than 30 ng/mL ($P < 0.001$; odds ratio = 299) were independent malignant predictors in the subsequent multivariate analysis (Table 4).

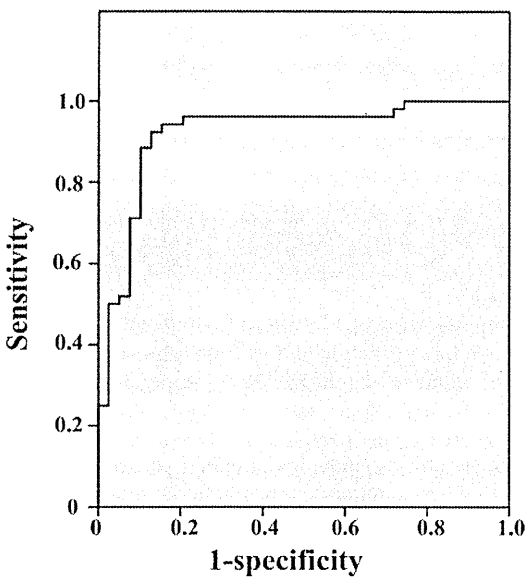

FIGURE 1. The receiver operating characteristic curve used to determine the optimal CEA cutoff levels in the pancreatic juice obtained by preoperative endoscopic retrograde pancreatography for the prediction of the malignancy of branch duct type IPMN. The area under the curve for the CEA levels in the pancreatic juice was 0.92, and the determined cutoff level for differentiation between benign and malignant IPMNs was 30 ng/mL.

TABLE 2. The Diagnostic Cutoff Levels of the Tumor Size, Main Duct Size, Mural Nodule Size, and CEA Levels in the Pancreatic Juice for Differentiating Between Benign and Malignant IPMN Based on the Receiver Operating Characteristic Curves

	Area Under Curve	Cutoff Value
Tumor size	0.612	30 mm
Main pancreatic duct size	0.711	5 mm
Mural nodule size	0.819	5 mm
CEA levels in the pancreatic juice*	0.920	30 ng/mL

*The CEA in the pancreatic juice could be measured in 91 patients who received preoperative ERP.

With regard to the mural nodule size, the sensitivity, specificity, and accuracy of the cutoff (5 mm) for differentiating between benign and malignant IPMN were 74.4%, 80.4%, and 76.9%, respectively and those for the CEA cutoff level in the pancreatic juice (30 ng/mL) were 94.2%, 84.6%, and 90.1%, respectively.

We found that mural nodule size determined by EUS and CEA levels in the pancreatic juice were significantly correlated ($P < 0.001$; Table 5). There were 5 patients with just 5 mm of mural nodule with a CEA level in the pancreatic juice higher than 30 ng/mL, and they included 4 patients with adenoma and 1 patient with CIS.

Combination Analysis of the Mural Nodule Size and CEA Level in the Pancreatic Juice

If the analyses of the mural nodule size and CEA level in the pancreatic juice were combined, all patients with a mural nodule size larger than 5 mm who also had a CEA level in the pancreatic juice higher than 30 ng/mL had malignancy, indicating that the positive predictive value of both a mural nodule larger than 5 mm and a CEA level in the pancreatic juice higher than 30 ng/mL was 100%. Moreover, 26 patients of the 27 patients with a mural nodule size larger than 5 mm and a CEA level in the pancreatic juice higher than 30 ng/mL had benign IPMN, indicating that the negative predictive value of both a mural nodule size larger than 5 mm or a CEA level in the pancreatic juice higher than 30 ng/mL was 96.3% (Fig. 2).

DISCUSSION

Surgical resection offers the best chance for a cure for the patients with IPMN; however, observation may be a better management strategy for the patients with a low risk of malignancy, because a pancreatectomy is an invasive procedure, especially in elderly patients.[16] Therefore, many investigators have performed studies to identify factors that can be used to predict the likelihood of malignancy in the patients with IPMNs. Most clinicians have agreed that the main duct type IPMN has high malignant potential, and surgical resection is recommended for all patients with main duct type IPMN.[4–6,10] However, there is still no definite management consensus, including the surgical indications, for patients with branch duct type IPMN, because the malignant potential of branch duct type IPMN is relatively low.[10–14] Thus, it is necessary to identify more accurate factors that can predict the malignancy and determine the indications for surgical resection for the patients with the branch duct type IPMN.

The International Consensus Guidelines have put forward an algorithm for the surgical management of branch duct type IPMN, which is based on the tumor size, patient symptoms, and "high risk stigmata" (mural nodule and positive cytology in the pancreatic juice).[17] Several recent studies reported that the size of mural nodules was a more significant malignant factor than the tumor size for predicting the malignancy of branch duct type IPMN.[6,10,12,14] In addition, the MPD size, positive EUS fine-needle aspiration (FNA) cytology, and high CEA or carbohydrate antigen (CA)72.4 levels in the cystic fluid have been reported to be factors that can be used to predict the malignancy of branch duct type IPMN.[5,18–21] However, the accuracies of these factors were not high enough to distinguish between benign and malignant IPMNs. Moreover, the cytology of the pancreatic juice should be a criterion standard for the preoperative pathological diagnosis. However, the sensitivity of preoperative cytology was only 11.1% in this series. Therefore, we tried to identify more accurate predictors of the malignant potential of branch duct IPMN to determine an optimal management consensus. If CIS could be determined for the patients with branch duct type IPMN by several parameters, that would be powerful. However, in this study, the number of CIS was small; only 41 patients. Therefore, we could not analyze separately in each group. In the future, we would like to try

TABLE 3. The Results of the Univariate Analysis of the Malignant Predictive Factors for Branch Duct Type IPMN

	Benign (n = 56), n (%)	Malignant (n = 78), n (%)	*P*
Age, >70 yr	25/56 (44.6%)	44/78 (56.4%)	0.179
Sex, male	30/56 (53.6%)	44/78 (56.4%)	0.745
Symptom	27/56 (48.2%)	46/78 (59%)	0.217
Jaundice	0 (0%)	14 (18%)	<0.001
Body weight loss	5 (8.9%)	11 (14.1%)	0.362
Abdominal pain	14 (25%)	23 (29.5%)	0.567
Back pain	9 (16.1%)	9 (11.5%)	0.448
Onset or worsening of diabetes mellitus	13/56 (23.2%)	26/78 (33.3%)	0.203
Tumor occupied location, head	35/56 (62.5%)	65/78 (83.3%)	0.006
Tumor size, >30 mm	20/56 (35.7%)	37/78 (47.4%)	0.176
Main pancreatic duct size, >5 mm	16/56 (28.6%)	52/78 (66.7%)	<0.001
Mural nodule size, >5 mm	11/56 (19.6%)	57/78 (73.1%)	<0.001
Serum CEA, elevated	3/56 (5.4%)	9/78 (11.5%)	0.217
Serum CA19–9, elevated	6/56 (10.7%)	27/78 (34.6%)	0.002
Cytology in the pancreatic juice,* class IV or V	0/44 (0%)	6/54 (11.1%)	0.023
CEA levels in the pancreatic juice,† >30 ng/m	6/39 (15.4%)	49/52 (94.2%)	<0.001

*Cytological examination of the pancreatic juice was possible in 98 patients.
†The CEA in the pancreatic juice could be measured in 91 patients.

TABLE 4. The Results of the Multivariate Analysis of the Malignant Predictive Factors for Branch Duct Type IPMN

	P	Odds Ratio	95% Confidence Interval
Jaundice	0.989		
Tumor occupied location, head	0.136		
Main pancreatic duct size, >5 mm	0.082		
Mural nodule size, >5 mm	0.003	12.9	2.38–70.3
Serum CA19–9, elevated	0.803		
Cytology in the pancreatic, class IV or V	0.983		
CEA levels in the pancreatic juice, >30 ng/mL	<0.001	299	17.7–5067

TABLE 5. Correlation Between Findings of EUS and CEA in the Pancreatic Juice Obtained by ERP for the Patients With Branch Duct Type IPMN

EUS Findings (Mural Nodule Size)	CEA Levels in the Pancreatic Juice Obtained by ERP		
	≤30 ng/mL (n = 36)	>30 ng/mL (n = 55)	*P*
≤5 mm (n = 45)	27	18	<0.001
>5 mm (n = 46)	9	37	

to analyze by clustering the patients with branch duct type IPMN into 3 groups—adenoma, CIS, and invasive IPMC.

In this study, we defined branch duct type IPMN as that with cyst formation caused by BPD dilation with or without MPD dilation. The reasons that we included mixed type IPMN into the branch duct type IPMN are as follows:

1. It is difficult to distinguish branch duct type IPMN with MPD dilatation caused by outflow of copious mucin from a side branch cyst from the mixed type IPMN with MPD dilatation resulting from the production of mucin in the MPD,[6] by preoperative radiological imaging.
2. Branch duct type IPMN sometimes has microscopic involvement into the MPD without radiological evidence of dilatation of the MPD; however, the preoperative prediction of this phenomenon is impossible.
3. The malignant potential of mixed type IPMN was reported to be lower than that of the main duct type,[6] although there have been a limited number of reports about the potential of mixed type IPMN.

Indeed, in this study, we found 22 patients with branch duct IPMN with MPD dilation, ie, mixed type on imaging findings (the pathological diagnosis in branch pancreatic duct is 5 adenoma, 10 CIS, and 7 invasive IPMC). In 5 mixed type IPMN patients with adenoma, only 1 patient had an adenoma in MPD. Remaining 4 patients had no atypia in MPD, which had the secondary dilation of MPD because of inflow of mucinous fluid from cystic branch duct. Thus, it is very difficult to distinguish branch duct type IPMN from mixed type IPMN by radiological imaging, because we could not predict microscopic involvement into MPD in mixed type IPMN patients.

For this study, we reanalyzed the cutoff values for the tumor size, MPD size, mural nodule size, and CEA level in the pancreatic juice to distinguish between benign and malignant IPMN exclusively in patients with branch duct type IPMN, using ROC curves. Our results suggested that a mural nodule size larger than 5 mm and a CEA level in the pancreatic juice obtained by preoperative ERP higher than 30 ng/mL were independent significant predictors of malignancy in a multivariate analysis. In several significant malignant predictors for branch duct type IPMN on univariate analysis, but not significant on multivariate analysis, we found jaundice, MPD dilation, and elevated serum CA19–9 as malignant predictive factors for IPMN.[10–14] All 8 branch duct type IPMN patients with jaundice, MPD dilation, and elevated serum CA19–9 had malignancy, whereas in 32 patients without jaundice, MPD dilation or elevated serum CA19–9, 10 patients had malignancy with a high CEA in the pancreatic juice. Therefore, the branch duct type IPMN patients with jaundice, MPD dilation, and elevated serum CA19–9 may not require ERP, because the positive predictive values for malignancy of combination of these 3 factors are high, whereas ERP may be useful procedure to distinguish between

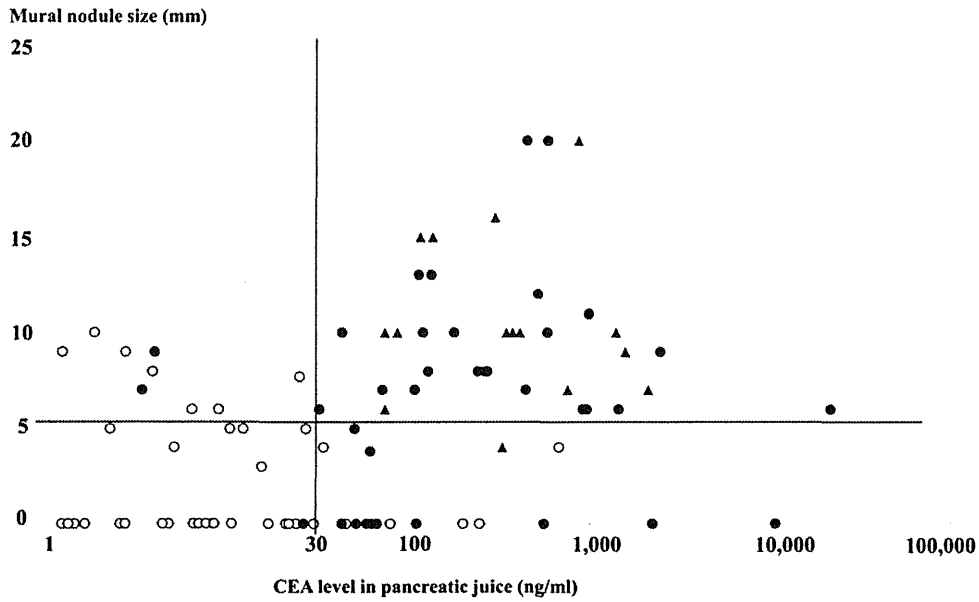

FIGURE 2. The distribution of the mural nodule size and CEA levels in the pancreatic juice in patients with branch duct type IPMN. IPMNs classified as adenoma and borderline neoplasm are indicated by white circles (○), carcinoma in situ by black circles (●), and invasive IPMC by black triangles (▲). All patients (100%) with a mural nodule size larger than 5 mm and a CEA level in the pancreatic juice higher than 30 ng/mL had malignant IPMN, whereas only 1 patient among 27 with a mural nodule size ≤5 mm and a CEA level in the pancreatic juice 30 ng/mL or lower had malignant IPMN.

benign and malignant IPMNs for patients without jaundice, MPD dilation, nor elevated serum CA19–9.

We previously reported that the cutoff value for the CEA level in the pancreatic juice to distinguish malignant from benign IPMN was 110 ng/mL for the patients with all types IPMN,[2] whereas this study suggested that the cutoff value was 30 ng/mL for the patients with branch duct type IPMN. It is considered that the CEA levels in main duct type IPMN are higher than those of other types of IPMN, because the CEA levels of the pancreatic juice obtained from the MPD reflect the direct secretion of CEA for the main duct type, whereas the CEA levels for the branch duct type IPMN reflect the outflow into the MPD from cystic side branch secretions.

Recently, measurements of CEA or/and CA72.4 in the cystic fluid obtained by EUS-FNA were reported to be useful for the differentiation of malignant from benign IPMN.[20] In our institute, we have measured the CEA levels in the pancreatic juice obtained from the MPD by preoperative ERP in the patients with all types IPMN, but not in the cyst fluid obtained by EUS-FNA, because (1) obtaining pancreatic juice by ERP is not associated with any risk of peritoneal seeding, and actually, peritoneal seeding was not found in all patients, whose pancreatic juice obtained by preoperative ERP, and (2) the branch duct type IPMNs are often consisted of multilocular cysts, and it is unknown which cyst has the most severe atypia, whereas the pancreatic juice in the MPD obtained by ERP includes secreted CEA from all of the pancreatic ducts. However, further studies of the evaluation of the correlations between the CEA levels in the pancreatic juice in the MPD and the CEA levels in the cyst fluid should be performed.

In this study, there were 29 patients with a mural nodule size 5 mm or smaller and a tumor size 30 mm or larger, who were predicted to have benign IPMN by findings of EUS and CT. Among 29 patients, we had 8 malignant IPMN patients with a CEA level in the pancreatic juice obtained by ERP more than 30 ng/mL. Furthermore, in 23 patients with branch duct type IPMN without a mural nodule and a tumor size 30 mm or smaller, 6 patients had malignancy with a CEA level in the pancreatic juice higher than 30 ng/mL. These results suggest that ERP may be a useful procedure for some branch duct type IPMN patients with a mural nodule size 5 mm or smaller and a tumor size 30 mm or smaller, whereas we cannot clarify which types of patients would be benefited from this additional invasive procedure.

When the combination of a mural nodule size larger than 5 mm and a CEA level in the pancreatic juice higher than 30 ng/mL is used, the predictive value is excellent (100%), indicating that branch duct type IPMN with a mural nodule size larger than 5 mm and a CEA level in the pancreatic juice higher than 30 ng/mL would be recommended for resection. Only 1 patient (1 of 27 patients) with a mural nodule size 5 mm or smaller and a CEA level in the pancreatic juice 30 ng/mL or lower had malignant IPMN, which suggests that the patients with branch duct type IPMN in this group might be better treated by strict observation.

In conclusion, we identified 2 useful predictive factors for malignancy in branch duct type IPMN; a mural nodule size larger than 5 mm and a CEA level in the pancreatic juice obtained by preoperative ERP more than 30 ng/mL. Additional studies in other populations will be needed to confirm the validity of our findings.

REFERENCES

1. Kloppel G, Solcia E, Longnecker DS, et al. *Histologic Typing of Tumors of the Exocrine Pancreas*. 2nd ed. Geneva, Switzerland: Springer-Verlag; 1996.
2. Kawai M, Uchiyama K, Tani M, et al. Clinicopathological features of malignant intraductal papillary mucinous tumors of the pancreas. *Arch Surg*. 2004;139:188–192.
3. Hirono S, Tani M, Kawai M, et al. Treatment strategy for intraductal papillary mucinous neoplasm of the pancreas based on malignant predictive factors. *Arch Surg*. 2009;144:345–349.
4. Jang JY, Hwang DW, Kim MA, et al. Analysis of prognostic factors and a proposed new classification for invasive papillary mucinous neoplasms. *Ann Surg Oncol*. 2011;18:644–650.

5. Murakami Y, Uemura K, Hayashidani Y, et al. Predictive factors of malignant or invasive intraductal papillary-mucinous neoplasms of the pancreas. *J Gastroitest Surg*. 2007;11:338–344.
6. Hwang DW, Jang JY, Lee SE, et al. Clinicopathologic analysis of surgically proven intraductal papillary mucinous neoplasms of the pancreas in SNUH: a 15-year experience at a single academic institution. *Langenbecks Arch Surg*. 2012;397:93–102.
7. Wasif N, Bentrem DJ, Farrell JJ, et al. Invasive intraductal papillary mucinous neoplasm versus sporadic pancreatic adenocarcinoma. *Cancer*. 2010;116:3369–3377.
8. Poultsides GA, Reddy S, Cameron JL, et al. Histopathologic basis for the favorable survival after resection of intraductal papillary mucinous neoplasm-associated invasive adenocarcinoma of the pancreas. *Ann Surg*. 2010;251:470–476.
9. Yopp AC, Katabi N, Janakos M, et al. Invasive carcinoma arising in intraductal papillary mucinous neoplasms of the pancreas. A matched control study with conventional pancreatic ductal adenocarcinoma. *Ann Surg*. 2011;253:968–974.
10. Schmidt CM, White PB, Waters JA, et al. Intraductal papillary mucinous neoplasms. Predictors of malignant and invasive pathology. *Ann Surg*. 2007;246:644–654.
11. Jang JY, Kim SW, Lee SE, et al. Treatment guidelines for branch duct type intraductal papillary mucinous neoplasms of the pancreas: when can we operate or observe? *Ann Surg Oncol*. 2007;15:199–205.
12. Akita H, Takeda Y, Hoshino H, et al. Mural nodule in branch duct-type intraductal papillary mucinous neoplasms of the pancreas is a marker of malignant transformation and indication for surgery. *Am J Surg*. 2011;202:214–219.
13. Shimizu Y, Kanemitsu Y, Sano T, et al. A nomogram for predicting the probability of carcinoma in patients with intraductal papillary mucinous neoplasm. *World J Surg*. 2010;34:2932–2938.
14. Salvia R, Crippa S, Falconi M, et al. Branch-duct intraductal papillary mucinous neoplasms of the pancreas: to operate or not to operate? *Gut*. 2007;56:1086–1090.
15. Cotton PB, Lehman G, Vennes J, et al. Endoscopic sphincterotomy complications and their management: an attempt at consensus. *Gastrointest Endosc*. 1991;37:383–393.
16. Weinberg BM, Spiegel BMR, Tomlinson JS, et al. Asymptomatic pancreatic cyst neoplasms: maximizing survival and quality of life using Markov-based clinical nomograms. *Gastroenterology*. 2010;138:531–540.
17. Tanaka M, Chari S, Adsay V, et al. International consensus guidelines for management of intraductal papillary mucinous neoplasms and mucinous cystic neoplasms of the pancreas. *Pancreatology*. 2006;6:17–32.
18. Maker AV, Lee LS, Raut CP, et al. Cytology from pancreatic cysts has marginal utility in surgical decision-making. *Ann Surg Oncol*. 2008;15:3187–3192.
19. Paris SA, Attasaranya S, Leblanc JK, et al. Role of endoscopic ultrasound in the diagnosis of intraductal papillary mucinous neoplasms: correlation with surgical histopathology. *Clin Gastroenterol Hepatol*. 2007;5:489–495.
20. Maire F, Voitot H, Aubert A, et al. Intraductal papillary mucinous neoplasms of the pancreas: performance of pancreatic fluid analysis for positive diagnosis and the prediction of malignancy. *Am J Gasetroenterol*. 2008;103:2871–2877.
21. Jong K, Poley JW, Hooft JE, et al. Endoscopic ultrasound-guided fine-needle aspiration of pancreatic cyst lesions provides inadequate material for cytology and laboratory analysis: initial results from a prospective study. *Endoscopy*. 2011;43:585–590.

Cancer Science
The official journal of the Japanese Cancer Association JCA

Review Article

Epithelial–mesenchymal transition in cancer development and its clinical significance

Masaaki Iwatsuki,[1,2] Koshi Mimori,[1] Takehiko Yokobori,[1] Hideshi Ishi,[1,3] Toru Beppu,[2] Shoji Nakamori,[4] Hideo Baba[2] and Masaki Mori[1,3,5]

[1]Department of Surgical Oncology, Medical Institute of Bioregulation, Kyushu University, Beppu; [2]Department of Gastroenterological Surgery, Graduate School of Medical Sciences, Kumamoto University, Kumamoto; [3]Department of Gastroenterological Surgery, Graduate School of Medicine, Osaka University, Osaka; [4]Department of Surgery, Osaka National Hospital, Osaka, Japan

(Received September 07, 2009/Revised October 21, 2009/Accepted October 21, 2009/Online publication November 24, 2009)

The epithelial–mesenchymal transition (EMT) plays a critical role in embryonic development. EMT is also involved in cancer progression and metastasis and it is probable that a common molecular mechanism is shared by these processes. Cancer cells undergoing EMT can acquire invasive properties and enter the surrounding stroma, resulting in the creation of a favorable microenvironment for cancer progression and metastasis. Furthermore, the acquisition of EMT features has been associated with chemoresistance which could give rise to recurrence and metastasis after standard chemotherapeutic treatment. Thus, EMT could be closely involved in carcinogenesis, invasion, metastasis, recurrence, and chemoresistance. Research into EMT and its role in cancer pathogenesis has progressed rapidly and it is now hypothesized that novel concepts such as cancer stem cells and microRNA could be involved in EMT. However, the involvement of EMT varies greatly among cancer types, and much remains to be learned. In this review, we present recent findings regarding the involvement of EMT in cancer progression and metastasis and provide a perspective from clinical and translational viewpoints. (*Cancer Sci* 2010; 101: 293–299)

Development of distant metastases is the final stage of solid cancer progression and is responsible for the majority of cancer-related deaths.[1] Distant metastasis alone or with concurrent locoregional recurrence accounts for nearly 80% of all first relapses in women with breast cancer.[2] While clinically of great importance, the biology of metastasis remains unsolved. The process of tumor metastasis consists of multiple steps, all of which are required to achieve tumor spreading.[3,4] First, cancer cells escape from the primary tumor site. Next, cancer cells invade the tumor stroma and enter the blood circulation directly or the lymphatic system via intravasation. Most circulating cancer cells undergo apoptosis due to anoikis conditions.[5] If cancer cells survive in circulation they may reach more suitable sites by attaching to endothelial cells and extravasating from the circulation into the surrounding tissues. Finally, distal colonization requires that cancer cells invade and grow in the new environment.

Recently, the concept of the epithelial–mesenchymal transition (EMT), as developed in the field of embryology, has been extended to cancer progression and metastasis.[6,7] *In vitro* and experimental animal model data now support the role of EMT in metastasis, concepts supported by analyses of clinical samples. Indeed, the biology of EMT has been clarified in tumor samples through use of EMT-associated markers, such as mesenchymal-specific markers (i.e. vimentin and fibronectin),[8,9] epithelial specific markers (i.e. E-cadherin and cytokeratin),[10,11] and transcription factors (i.e. SNAIL and SLUG).[12]

Most recently, several intriguing studies have described the novel mechanism underlying EMT activation. In the current study, we will discuss the role of small non-coding RNA (microRNA) in regulating EMT-related genes.[13–15] Furthermore, Mani *et al.* disclosed that EMT could generate breast cancer cells with stem cell-like characteristics.[16] Here, we update and discuss recent progress in studies of EMT. These new data improve our understanding of the mechanisms of cancer progression and metastasis as well as therapy resistance. This new information may lead to development of novel clinical targets and improve the clinical management of cancer patients.

Involvement of EMT in Cancer Progression

In the 1980s, Greenburg and Hey first analyzed EMT-associated changes in cell phenotype and mesenchymal states in adult and embryonic epithelia.[17] EMT and the inverse process of mesenchymal–epithelial transition (MET) are major embryological mechanisms for tissue remodeling, as in gastrulation and segment formation.[18] The process of EMT consists of multiple steps.[19,20] First, cell–cell adhesion disintegrates with the loss of epithelial markers such as E-cadherin and the gain of mesenchymal markers such as vimentin. Next, there is a loss of basoapical polarization and the acquisition of front-rear polarization. Then, the cytoskeleton undergoes remodeling, with changes in cortical actin and actin stress fibers. Finally, cell-matrix adhesion is altered, with activation of proteolytic enzymes such as matrix metalloproteases. Note that the process of metastasis in epithelial cancer also consists of multiple steps.[3,4] That is, cells detach from the primary tumor and invade the surrounding tumor stroma. They subsequently enter into the circulation and reach new metastatic sites. Therefore, the process of EMT during cancer progression and metastasis closely resembles that observed in embryologic development. Accordingly, molecular analyses based on EMT in embryology have been applied to cancer progression.

In the 1990s, accumulating evidence indicated that EMT was associated with cancer progression.[7] Indeed, these transformations may be associated with EMT-related signal pathways during development.[7,21] However, Boyer *et al.* stated that EMT during development depends on additional activities of distinct and specific signaling molecules which are highly controlled spatially and temporally, and which do not occur under normal circumstances. On the other hand, EMT in cancer progression could be due to autonomous oncogenic activation of signaling molecules without additional stimulation.[22] Therefore,

[5]To whom correspondence should be addressed.
E-mail: mmori@gesurg.med.osaka-u.ac.jp

doi: 10.1111/j.1349-7006.2009.01419.x

comparisons of EMT signaling pathways in embryological development and cancer progression may make it possible to identify novel pathways specific to cancer progression and to suggest new therapeutic strategies in cancer therapy.[23]

The Molecular Mechanism of EMT in Cancer Progression

Multiple complex signaling systems are required for induction of EMT because epithelial cells undergoing EMT must undergo both functional and morphologic changes. Studies of the crosstalk among the intracellular signal networks could help us to understand the mechanisms regulating EMT. Here, we discuss the regulation of representative molecules, E-cadherin, a major EMT inducer, transforming growth factor-β (TGF-β) signal pathways, and microRNA regulation reported in recent studies (Fig. 1).

E-cadherin regulation. One of the characteristic findings in EMT is the loss of cell–cell adhesion with diminished expression of E-cadherin. E-cadherin, a calcium-dependent transmembrane glycoprotein expressed in most epithelial tissues, constructs a tight junction which connects adjacent cells. The loss of E-cadherin can lead to tumor progression, metastasis, and poorer prognosis in various human carcinomas.[10,11,24,25] Genetic or epigenetic alterations cause a functional loss of E-cadherin. For instance, mutations in E-cadherin are found in diffuse gastric cancer[26] and lobular breast carcinoma.[27] In addition, hypermethylation of the E-cadherin promoter region is found in various human carcinomas, resulting in frequent loss of E-cadherin expression.[28,29] Interestingly, Graff *et al.* proposed that the degree of methylation of the E-cadherin promoter region during metastatic progression is unstable and heterogeneous.[28] This finding suggests that the loss of E-cadherin by methylation in a primary lesion may drive metastatic progression, indicating that EMT is involved in cancer metastasis. Besides genetic or epigenetic control, E-cadherin is regulated by various signal networks, such as TGF-β signaling and transcription factors as discussed in more detail below.

TGF-β signaling. Miettinen *et al.* first revealed that TGF-β induced EMT in normal mammary epithelial cells.[30] In fact, TGF-β is an important inducer of EMT in cancer progression. However, TGF-β is well known to induce multiple responses in cancer progression.[31] For example, loss of the TGF-β signaling pathway results in the progression of cancer because TGF-β is a strong growth inhibitor.[32] Indeed, Hahn *et al.* reported that mutations in TGF-β and Smad4 give rise to pancreatic cancer[33] and colorectal cancer.[34] On the other hand, TGF-β can protect against apoptosis, and promote angiogenesis and immune suppression.[35] TGF-β induces EMT through multiple signal pathways, including direct phosphorylation of Smad 2 and Smad 3. As shown in Figure 1, TGF-β also activates other EMT-related signal pathways, including integrin, Notch, and Wnt signal pathways, all of which trigger EMT programs.

Transcription factors. Transcriptional repressors of E-cadherin such as zinc finger proteins (ZEB1, ZEB2), bHLH protein (Twist), and the snail family of zinc finger proteins (Snail, Slug) are associated with EMT.[36–40] As shown in Figure 1, various signal pathways such as TGF-β,[20] the Wnt cascade, and PI3K/AKT (phosphatidylinositol 3′ kinase–serine/threonine kinase) axis are connected with these transcriptional repressors of E-cadherin.[41] Recent studies have demonstrated that transcriptional repressors of E-cadherin are regulated by microRNAs as described below. Several transcriptional factors such as Snail, Slug, and Twist are useful markers to predict prognosis in various human carcinomas (Table 1). Peinado *et al.* proposed that E-cadherin repressors might participate in the process of EMT as follows. First, Snail and ZEB2 would initiate down-regulation of E-cadherin. Then, Slug and ZEB1 would maintain repression of E-cadherin.[42] However, the effect of E-cadherin repressors on mesenchymal markers such as vimentin and N-cadherin remains unsolved.

Regulation of EMT by microRNA. Recent studies of small non-coding RNAs are shedding light on the regulation of gene expression and proteins in metastasis. It was shown that miR-10b overexpression is associated with invasiveness and metastatic potential.[43] miR-10b is overexpressed in metastatic breast cancer, and up-regulated by EMT transcription factor Twist. Recent independent studies revealed that the miR-200 family (miR-200a, miR-200b, miR-200c, miR-141, and miR-429) and miR-205 play critical roles in regulating EMT, targeting the E-cadherin repressors ZEB1 and ZEB2.[13,15] Gibbons *et al.* found that metastasis-prone tumor cells established from

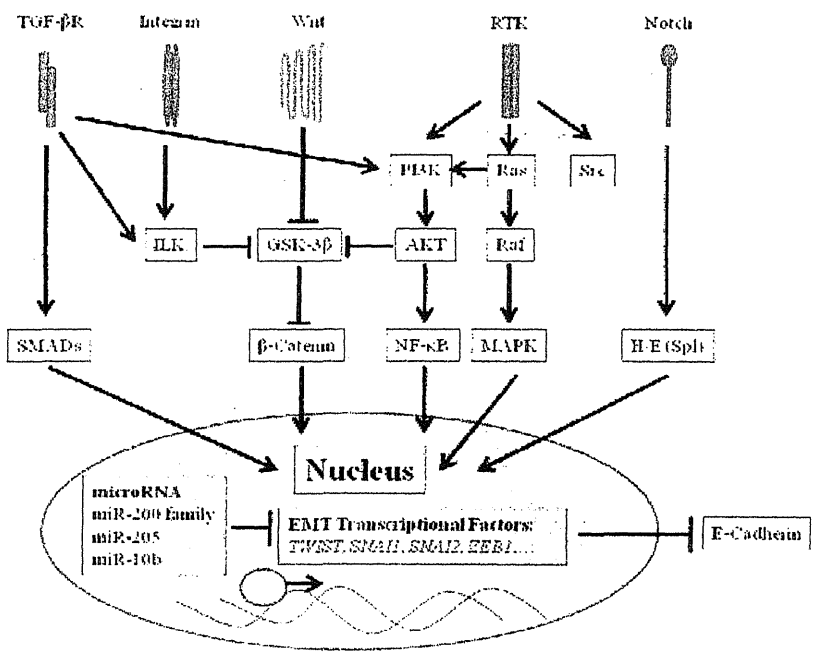

Fig. 1. Depiction of signal pathways regulating the epithelial–mesenchymal transition (EMT). Selected signal pathways regulating E-cadherin are schematized. Transforming growth factor (TGF)-β signals toward the SMAD pathway or the PI3K/AKT axis. Wnt ligands block β-catenin degradation. Excess β-catenin enters the nucleus and upregulates *SLUG* and *SNAIL* transcription. In integrin signaling, overexpression of ILK leads to nuclear translocation of β-catenin. Signals via RTK lead to EMT through the Ras-Raf-MAPK pathway or the PI3K/AKT pathway. AKT, serine/threonine kinase; GSK-3β, glycogen synthase kinase-3β; H/E (Spl), Hairy and enhancer of split; ILK, integrin-linked kinase; MAPK, mitogen-activated protein kinase; NF-κB, nuclear factor-κB; PI3K, phosphatidylinositol 3′ kinase; RTK, receptor tyrosine kinase; TGF-βR, transforming growth factor-β receptor.

doi: 10.1111/j.1349-7006.2009.01419.x